Semi-Solid Extrusion 3D Printing of Tailored ChewTs for Veterinary Use - A Focus on Spectrophotometric Quantification of Gabapentin

Sjöholm, Erica; Mathiyalagan, Rathna; Lindfors, Lisa; Wang, Xiaoju; Ojala, Samuli; Sandler, Niklas

Published in:
European Journal of Pharmaceutical Sciences

DOI:
10.1016/j.ejps.2022.106190

Published: 01/01/2022

Document Version
Final published version

European Journal of Pharmaceutical Sciences 174 (2022) 106190

Contents lists available at ScienceDirect

European Journal of Pharmaceutical Sciences

journal homepage: www.elsevier.com/locate/ejps

Semi-solid extrusion 3D printing of tailored ChewTs for veterinary use - A focus on spectrophotometric quantification of gabapentin

Erica Sjöholm [a,*], Rathna Mathiyalagan [a], Lisa Lindfors [a], Xiaoju Wang [a], Samuli Ojala [b], Niklas Sandler [a,c]

[a] Pharmaceutical Sciences Laboratory, Faculty of Science and Engineering, Åbo Akademi University, Tykistökatu 6A, 20520 Turku, Finland
[b] Oulun Keskus Apteekki, Isokatu 45, 90100 Oulu, Finland
[c] Nanoform Finland Oyj, Viikinkaari 4, 00790 Helsinki, Finland

ARTICLE INFO

Keywords:
Semi-solid extrusion 3D printing
Drug delivery
Tailored dosage forms
Veterinary medicine
Gabapentin
UV-Vis spectrophotometric quantification
Chewable tablets

ABSTRACT

Currently, there are a few or none marketed gabapentin veterinary products, leading to treatment with compounded dosage forms or off-label use of human-marketed products. With the said approaches, there are significant risks of preparation errors, rendering these practices suboptimal. A new manufacturing technique to accurately and rapidly prepare veterinary dosage forms close to the point-of-care is needed. However, a current hurdle in developing small-dose gabapentin dosage forms is the quantification of the gabapentin molecule. UV–Vis spectrophotometric quantification possesses suitable properties for implementation at small production sites, but quantifying gabapentin with the said technique has proven to be challenging as the small molecule lacks chromophores. This study aimed at thoroughly assessing UV–Vis spectrophotometric gabapentin quantification methods with the intent of finding a reliable method. Excellent linearity ($R^2 = 0.9998$) in a broad and useful concentration range (0.5–40 μg/mL) was detected for the ascorbic acid derivatization method at a wavelength of 376 nm. The method was successfully applied to determine the drug content in the prepared semi-solid extrusion 3D-printed dosage forms. This study proved that pet-friendly tailored gabapentin dosage forms could easily be manufactured by semi-solid extrusion 3D printing and UV–Vis spectrophotometrically analyzed with the ascorbic acid derivatization method.

1. Introduction

Gabapentin (GBP) is an anticonvulsant used for seizure prevention in epilepsy patients (Taylor, 2002). It is also commonly utilized in the treatment of neuropathic pain, a type of pain resulting from damage to the nervous system (Brannagan, 2009). Epilepsy and neuropathic pain are not only a concern for humans, but also animals suffer these conditions. GBP has become a part of established clinical practice in the treatment of neuropathic pain or preventing seizures in cats and dogs (Mathews et al., 2014). Recommended doses for dogs start at 10 mg/kg two to three times daily, and for cats, 5 mg/kg twice daily. Dose titration is often necessary to find an effective dose and reduce the risk of adverse reactions when using GBP, as well as gradual discontinuation of the medication is recommended (Mathews et al., 2014). These regimens mean that a significant number of veterinary patients need to be treated with very small (and often varying) doses of GBP. However, since there is no or only a limited amount of market-approved veterinary GBP dosage forms, many pets are thus currently treated off-label with human-marketed GBP dosage forms. This means that the pet owners themselves are responsible for splitting tablets or dividing capsules into appropriate doses. Dividing dosage forms involves a risk of under- or overdosing as it is difficult to obtain uniform doses (McDevitt et al., 1998). Another means of providing suitable drug doses for animals is compounding. However, the current compounding practice is often unsatisfactory due to compliance issues and risks of preparation errors (Davidson, 2017). A new way of compounding GBP and other drugs for veterinary use is needed to achieve the best possible compliance, bioavailability, and therapeutic effect in small pets.

There are, however, challenges in the development of GBP dosage forms, i.e., reliable identification and quantification of the GBP molecule. There are several techniques that have been utilized for the quantification of zwitterionic epilepsy drugs such as GBP, but according

* Corresponding author at: Pharmaceutical Sciences Laboratory, Faculty of Science and Engineering, Åbo Akademi University, Tykistökatu 6A, 20520 Turku, Finland.
E-mail address: erica.sjoholm@abo.fi (E. Sjöholm).

https://doi.org/10.1016/j.ejps.2022.106190
Received 3 November 2021; Received in revised form 28 February 2022; Accepted 12 April 2022
Available online 17 April 2022

to Kostić et al., ultraviolet-visible (UV–Vis) spectrophotometry is the most utilized (Kostić et al., 2014). UV–Vis spectrophotometry possesses many advantages over the other quantification techniques, i.e., low cost, good performance, and simplicity of the procedure, making it the preferred technique for quantifying GBP and suitable for analysis of compounded dosage forms close to the point-of-care (Almasri et al., 2019).

Whereas many molecules can be directly analyzed without further derivatization, the GBP molecule lacks significant absorbance in the UV–Vis wavelength range. Thus, numerous methods have been developed to determine GBP in bulk, dosage forms, and human or environmental samples. Many methods involve derivatization of the molecule in order to obtain a measurable complex. The challenge of quantifying GBP has been addressed in the literature, and several theoretical comparisons have been conducted (Kostić et al., 2014; Abdulrahman and Basavaiah, 2011; Abdulrahman and Basavaiah, 2011; Gouda and Al Malah, 2013; Abdulrahman and Basavaiah, 2012), but only one practical comparison and assessment of different UV–Vis quantification methods has been published (Fonseca et al., 2017). In the study by Fonseca et al., three direct methods (no derivatization) and three derivatization methods were assessed together with one fluorometric method. To the best of the author's knowledge, more extensive comparative studies of various UV–Vis methods have not yet been published.

GBP can be found on the market as tablets, capsules, and liquids for the treatment of humans. Additionally, orodispersible films (Bhusnure et al., 2018), transdermal films (Sayare et al., 2019), and floating microspheres (Al-abadi and Rassol, 2011) have been investigated. Two compounding pharmacies in the US produce GBP dosage forms for veterinary use. The Golden Gate Veterinary Compounding Pharmacy produces capsules, flavored chewable tablets, micro tablets, and Q-tabs (Golden Gate Veterinary Compounding Pharmacy 2022). The Wedgewood Pharmacy provides chewable tablets and capsules (Wedgewood Pharmacy 2022). Pregabalin, a structural analog of GBP with highly similar physicochemical properties, has been FDM printed to produce intra-gastric floating controlled-release tablets (Lamichhane et al., 2019). The administration of solid dosage forms to animals is challenging, especially with a bitter-tasting drug as GBP. In order to circumvent the administration issues that arise in specific patient populations, including animals, that are reluctant to swallow intact tablets, chewable dosage forms can be prepared. A chewable tablet (ChewT) is an oral dosage form that is intended to be chewed prior to swallowing. Physical characteristics that need to be considered and assessed with ChewTs are hardness, chewability, size, disintegration in order to facilitate dissolution, and palatability (FDA, 2018). Palatability is the acceptance of the organoleptic properties, such as appearance, smell, taste, aftertaste, and mouth feel (e.g., texture). In order to facilitate administration, voluntary acceptance, which is the willingness of the animal to freely consume a product is ideal. To achieve acceptable palatability by dogs and cats, which is necessary for voluntary acceptance, the dosage form should not be too chewy, which is often the case for products prepared for pediatric use, and an animal-appropriate taste and scent enhancer should be added, preferably proteins of animal-origin (Nyamweya and Kimani, 2020; Aleo et al., 2018).

The conventional pharmaceutical manufacturing techniques are limited by the production of fixed doses in large batches. Alternatively, 3D printing offers the ability to on-demand produce dosage forms in small scale according to the needs of individual patients. The potential advantages associated with the use of 3D printing technologies in the development of medicines are evident and could solve the unmet need for several treatments, hence the US Food and Drug Administration (FDA) is encouraging the research to be continued within this area (Norman et al., 2017). In order to automate compounding close to the point-of-care, this study proposes the use of semi-solid extrusion (SSE) 3D printing for the production of ChewTs for veterinary use. SSE 3D printing is a material-extrusion technique that extrudes a pre-made gel or paste according to a pre-determined design in a layer-by-layer approach. Compared to FDM, the commonly investigated printing technique, SSE 3D printing does not require elevated temperatures making it suitable for temperature-sensitive drugs. SSE 3D printing has been investigated in several medical applications, such as patches (Andriotis et al., 2020; J. Liu et al., 2020; Noor et al., 2019), microneedle patches (Wu et al., 2020), scaffolds in bone tissue engineering (Bittner et al., 2019; K. Liu et al., 2020; Rasoulianboroujeni et al., 2019; Zhou et al., 2020), human organs (Noor et al., 2019), and microfluidic devices (Ching et al., 2019). Lately, SSE 3D printing has also gained interest towards the production of drug-loaded dosage forms for humans and animals. This technique has been utilized to prepare immediate release tablets (El Aita et al., 2019; Conceição et al., 2019; Croitoru-Sadger et al., 2019; Cui et al., 2020; Dores et al., 2020; Eduardo et al., 2021; Yang et al., 2020; Zheng et al., 2020), controlled release tablets (El Aita et al., 2020; Cheng et al., 2020; Cui et al., 2019; Yang et al., 2020), poly pills (Haring et al., 2018; Siyawamwaya et al., 2019), chewable printlets (Goyanes et al., 2019; Herrada-Manchón et al., 2020; Karavasili et al., 2020; Rycerz et al., 2019; Tagami et al., 2021), and orodispersible films (Elbl et al., 2020; Sjöholm et al., 2020; Yan et al., 2020). GBP-containing ChewTs by means of printing have not, to the best of the authors knowledge, been explored previously.

In 2015, FDA approved the first 3D printed tablet, Spritam, and it is still the only 3D printed tablet with FDA approval. This tablet is produced by Aprecia Pharmaceuticals by their proprietary ZipDose® Technology platform and is an orodispersible dosage form that rapidly disintegrates in the mouth with a sip of water (Eisenstein, 2015). In 2021, the Chinese pharmaceutical and 3D printing technology company Triastek received an Investigational New Drug (IND) approval from FDA for its first 3D-printed drug product, T19. Triastek utilizes Melt Extrusion Deposition (MED) technology to 3D print T19 for the treatment of rheumatoid arthritis (Everett, 2021). Despite the high amount of research being conducted within this area, FDA do yet not have a particular guidance regarding printing of drugs and biologics, but the FDA's center for Drug Evaluation and Research (CDER) has acknowledged the role of 3D printing in developing drugs and encourages pharmaceutical companies to use this technology. A guidance regarding 3D printing of medical devices was released by the FDA in 2017 (U.S. Food and Drug Administration, Statement by FDA Commissioner Scott Gottlieb 2017). In the European Union there is currently no specific guidelines for 3D-printed products, only for the machinery itself.

The ultimate goal of this study was to improve tailored GBP treatment of pets by reducing the need for traditional compounding and off-label treatment with human medicines. This would improve drug safety, efficacy, and compliance in veterinary patients. To achieve this goal, this study aimed to find a simple, reliable, and inexpensive UV–Vis spectrophotometric method for quantification of GBP and to develop tailored SSE 3D-printed ChewTs for veterinary use.

2. Material

The pharmaceutical active ingredient gabapentin (GBP) from Fagron Services B.V. (Uitgeest, Netherlands) was kindly donated by Curify OY and used as received. Hydroxypropyl methylcellulose (HPMC) Methocel K3 Premium acts as a film-forming agent and was kindly donated by Dow Chemical Company (Bomlitz, Germany). The super disintegrant crospovidone (Kollidon CL) was kindly provided by BASF (Ludwigshafen, Germany), it was added to the printing ink in order to decrease the disintegration time. Mannitol (Ph. Eur.) was purchased from Merck (Darmstadt, Germany) and used in the formulation as a filling agent and for its suitability in chewable formulations, especially for its taste-masking properties. An 85% aqueous solution of glycerol from Fagron (Barsbüttel, Germany) was added for its plasticizing properties, and pure liver powder (LP) from CC Moore & Co. (Stalbridge, UK) was added for taste enhancement. Purified water (MQ) (Milli-Q®, Merck Millipore, Molsheim, France) and ethanol (Etax 94%, Altia Oyj, Rajamäki, Finland) were used as solvents.

The derivatization chemicals used for the quantification methods were L(+)-ascorbic acid (Riedel-de Haën, Sigma-Aldrich Laborchemikalien, Seelze, Germany), 2,4-dinitrophenol (Sigma-Aldrich, Steinheim, Germany; product of India), copper(II) chloride (Sigma-Aldrich, Steinheim, Germany; product of UK), chloranilic acid (Sigma-Aldrich, Steinheim, Germany; product of Austria), ninhydrin (Sigma-Aldrich, Steinheim, Germany; product of India), p-benzoquinone (Sigma-Aldrich, Steinheim, Germany), and vanillin (Sigma-Aldrich, Steinheim, Germany).

Besides purified water and ethanol, methanol (VWR Chemicals BDH, Fontenay-sous-Bois, France), N,N-dimethylformamide (DMF) (Sigma-Aldrich, Steinheim, Germany; product of France), dimethyl sulfoxide (DMSO) (Sigma-Aldrich, Steinheim, Germany; product of France), 37% hydrochloric acid (HCl) (Fisher Scientific, Loughborough, UK), dichloromethane (Sigma-Aldrich, Steinheim, Germany), acetonitrile (ACN) (Sigma-Aldrich, Steinheim, Germany; product of France), and acetaldehyde (Sigma-Aldrich, St. Louis, MO, USA) were utilized as solvents in the quantification study. Additionally, the following chemicals were used for the preparation of buffers: boric acid (Riedel-de Haën, Sigma-Aldrich Laborchemikalien, Seelze, Germany), sodium hydroxide (AnalaR NORMAPUR, VWR Chemicals BDH, Leuven, Belgium), sodium chloride (Sigma-Aldrich, St. Louis, MO, USA), disodium tetraborate decahydrate (Borax) (EMPROVE® ESSENTIAL, Merck, Darmstadt, Germany), disodium hydrogen phosphate (Fluka Analytical, Sigma-Aldrich, Steinheim, Germany), sodium dihydrogen phosphate (Sigma-Aldrich, Steinheim, Germany), and citric acid monohydrate (Sigma-Aldrich, St. Louis, MO, USA).

Purified water was used for analyses except for the measurement of the salivary pH, which was performed in sterile water (sterilized water by Fresenius Kabi Norway AS, Halden, Norway).

3. Methods

3.1. Spectrophotometric quantification of gabapentin

A central theme in the present study was to investigate gabapentin (GBP) quantification methods in order to find an easy and robust technique to be used in a clinical or a pharmacy setting. Thus, the literature was extensively searched for UV–Vis spectrophotometric quantification methods developed for, or tested on, pure GBP or dosage forms containing GBP. Quantification methods can roughly be divided into non-derivatization and derivatization-based methods; non-derivatization methods measure the native absorbance of the molecule in various solvents, while derivatization methods are based on coupling gabapentin with detection reagents. The methods were chosen based on certain criteria that would make them suitable to be used in a clinical or pharmacy setting. Firstly, the methods must be replicable, i.e., described clearly and in enough detail. Secondly, relatively rapid, and simple methods were preferred, and methods involving, for example, liquid-liquid extraction (separation) were discarded. Time-consuming methods spanning a whole day, or more, were excluded. Furthermore, the choice of solvent for gabapentin is highly relevant in terms of the applicability of a method to dissolution studies, and therefore, methods utilizing a gabapentin stock solution in water were preferred. As the GBP concentrations in dissolution samples are very low, the method must function in low ranges of analyte concentration. Thus, methods where the authors had proven linearity in concentrations <10 μg/ml were preferable. The economic aspect was also considered, and methods requiring expensive reagents were rejected. The price threshold was set to 80 € per reagent bottle. The methods included in the study are presented in Table 1, together with their assigned abbreviations. The ninhydrin methods were tested in different variations, which are labeled A, B, and C.

The methods were performed according to the respective authors' descriptions (see Table 1 and the summaries in Appendix I), except for the ninhydrin (NIN) and cupric chloride (CC) methods. In the two NIN methods the main difference between the published NIN derivatization methods, apart from the choice of solvent, is whether the samples are diluted with water to 10 mL before or after heating them. The variant where samples were diluted after heating was labeled A. In the published studies, the reaction volumes in the samples had not been adjusted to equal levels before heating. Since unequal proportions of reagent to reaction volume can potentially affect the accuracy and comparability of the results, a variant B was introduced, where all samples were adjusted to the same volume (ad 3 mL with purified water) before they were heated. The samples were then diluted to 10 mL after heating. In variant C, samples were diluted to 10 mL before heating. Different heating conditions for the NIN methods have also been

Table 1
Chosen quantification methods from the literature for assessment; detection wavelength (λ_{max}) and linear range as reported by the authors.

Method	Ref.	Reagent(s)	λ_{max} (nm)	Linear range (μg/mL)	Gabapentin solvent
MQ	(Fonseca et al., 2017; Gujral et al., 2009)	No derivatization; measurement of native absorbance in water	192 210	5.91–142.42 0.25–3.5	Water
MQ-ET	(Chandra Dinda et al., 2012; Fonseca et al., 2017)	No derivatization; measurement of native absorbance in water/ethanol	265 194	2–10 72.09–724.46	Water/ethanol
NIN-MET*	(Siddiqui et al., 2013)	Ninhydrin in methanol	575	10–30	Water
NIN-DMF*	(Abdellatef and Khalil, 2003; Galande et al., 2010)	Ninhydrin in N,N-dimethylformamide	569 405	40–280 50–300	Water
AA	(Adam et al., 2016)	Ascorbic acid in dimethyl sulfoxide	390, 531	12–60	Water
VAN7.5	(Abdellatef and Khalil, 2003; Fonseca et al., 2017; Kazemipour et al., 2013)	Duquenois reagent (vanillin, acetaldehyde, ethanol) + McIlvaine buffer (Na_2HPO_4, citric acid) with pH 7.5	376 392 402	80–360 64.25–712.08 10–90	Water
VAN8.5	(Kazemipour et al., 2013)	Duquenois reagent (vanillin, acetaldehyde, ethanol) + McIlvaine buffer (Na_2HPO_4, citric acid) with pH 8.5	402	10–90	Water
VAN—HCl	(Mohammed and Mohamed, 2015)	Vanillin in 1 M methanolic HCl	396	0.1–10	HCl/methanol
PBQ	(Abdellatef and Khalil, 2003; Fonseca et al., 2017)	*p*-benzoquinone in ethanol + phosphate buffer with pH 7.5	369 360	80–320 24.72–241.49	Water
CC	(Anis et al., 2011)	Cupric chloride in water + borate buffer with pH 7.5	246	40–95	Water
CHA	(Salem, 2008; Siddiqui et al., 2010)	Chloranilic acid in acetonitrile	535 314	60–200 6–30	Acetonitrile
DNP	(Abdulrahman and Basavaiah, 2011)	2,4-dinitrophenol in dichloromethane	420	2–18	Acetonitrile

*Ninhydrin derivatization was tested in three variants: A. Unequal reaction volumes, dilution after heating; B. Equal reaction volumes, dilution after heating; C. Dilution to set volume before heating.
MQ: purified water; ET: ethanol; MET: methanol; NIN: ninhydrin; AA: ascorbic acid; VAN: vanillin; HCl: hydrochloric acid; PBQ: p-benzoquinone; CC: cupric chloride; CHA: chloranilic acid; DNP: 2,4-dinitrophenol.

described in the literature, ranging between 70 °C for 15–80 min and 90 °C for 5 min (Abdellatef and Khalil, 2003; Galande et al., 2010; Siddiqui et al., 2010; Siddiqui et al., 2013). In this study, various conditions were tested: 70 °C for 80 min, 70 °C for 20 min, 80 °C for 10 min, and 90 °C for 5 min. The CC method described by Anis et al. is based on the formation of binary complexes between GBP and copper(II) ions (Anis et al., 2011). Based on the information given in the original article, it was assumed that the dilutions and measurements were carried out immediately without allowing for reaction time. When the method was initially tested according to this procedure, a detectable absorbance was not obtained in the majority of the samples. Therefore, the effect of different reaction times was investigated. After adding the borate buffer and the CC reagent to the stock solution aliquots, the samples were left to rest for 10, 15, 20, or 30 min before carrying out the final dilution to 10 mL, stopping the reaction. For all the methods, stock solutions, reagents, and buffers were prepared in volumetric flasks. Solutions were prepared fresh daily. Solid chemicals were accurately weighed with an analytical scale (AS 220.R2 PLUS by Radwag, Radom, Poland). All samples were prepared in 10 mL Falcon tubes. All volumes were calculated beforehand and accurately pipetted with manual single-channel pipettes (Rainin Pipet-Lite XLS by Mettler Toledo, Barcelona, Spain). After the addition of all chemicals, the Falcon tubes were mixed with a vortexer (Vortex Genie 2, Scientific industries, USA). For reactions involving heating, the samples were heated in a temperature-controlled water bath (Julabo SW22 by Julabo GmbH, Seelbach, Germany) and transferred into an ice bath immediately after heating to stop the reaction and speed up the cooling process. Absorbance measurements were carried out with a UV-6300 PC Double Beam Spectrophotometer (VWR International BVBA, Leuven, Belgium) capable of operating in a wavelength range of 190 to 1100 nm. The spectrophotometer was equipped with matching 10 mm quartz cells (QS High Precision Cell, Hellma Analytics, Müllheim, Germany). Data were gathered and analyzed with the UV–Vis Analyst software v. 5.44 (VWR International BVBA, Leuven, Belgium). The system was zero-calibrated with blank samples before the wavelength scans and the fixed wavelength measurements. All absorbances were measured against blank samples treated in the same way as the drug-containing samples.

The spectrophotometric quantification methods were first tested on pure GBP. Stock solutions of gabapentin were prepared, and series of dilutions were made to obtain working concentration ranges for the calibration curves. In accordance with the ICH guidance on linearity assessment, a minimum of five concentrations were incorporated into each calibration curve. The methods were also tested in broader concentration ranges which spanned beyond the linear ranges reported by the authors. Each method was tested on at least two different stock solutions on two separate days to evaluate the method's reproducibility under normally varying conditions. The most representative data from each method were analyzed with linear least squares regression performed with IBM® SPSS® Statistics v. 25, and the data were plotted with MagicPlot Student v. 2.9.1.

The methods exhibiting the best performance were tested on prepared gabapentin dosage forms to see whether the methods could be applied to the investigated formulations. This was performed by measuring the drug content of dosage forms containing a known theoretical drug amount. The procedure for drug content testing is described under 3.6.5.

3.1.1. Quantification method assessment

In order to determine how to assess the performance of the quantification methods, the validation criteria for the analytical methods were investigated. The author's decision was that the most relevant characteristics to compare in this context are the linearity, range, and precision of the methods. Furthermore, specificity in the form of an identification test can be observed in practice: a sample containing an analyte should give a positive absorbance reading, whereas a blank sample should give negligible to no absorbance readings.

3.2. Ink preparation

A semi-solid extrusion (SSE) 3D printing ink was prepared to develop tailored doses of gabapentin for veterinary use and to test the chosen quantification method's applicability to measure the gabapentin content in dosage forms. Several different ink formulations were investigated to find a suitable printing ink with a low enough viscosity to be prepared by hand and printed with an SSE 3D printer but high enough viscosity to keep the printed shape. Additionally, easy preparation of the printing ink is preferable in a clinical or pharmacy setting. Furthermore, the prepared printing ink cannot exhibit a change in viscosity over time, as this would affect the printing results, hence the rheology over time was assessed. Palatability is an important attribute of chewable dosage form in order to achieve voluntary acceptance in animals. GBP is known to be a bitter agent and additives are necessary to add to the formulation to mask the taste of the API. Mannitol is widely used as an excipient in chewable dosage forms for its non-hygroscopic nature, sweet flavor, and smooth consistency (Dahiya et al., 2015) and liver powder is generally liked by both cats and dogs as a flavoring agent. In order to prevent poor palatability of the dosage form, these two additives were added to the formulation.

The chosen printing ink for this study was an aqueous HPMC-based formulation that contained 20% GBP, 35% pre-made HPMC-gel (15% w/v), 27% mannitol, 6% crospovidone, 8% glycerol, 3% liver powder, and 1% purified water (all in w/w). The 15% (w/v) HPMC-gel was prepared 24 h prior to printing ink preparation. The HPMC-gel was prepared by mixing HPMC into 90 °C purified water (Tagami et al., 2019). The mixture was stirred for 2 min at 450 rpm in a 90 °C water bath, upon which the heat was turned off, and the solution was left to stir at 350 rpm for at least 1 h or until completely dissolved. A clear light-green solution was obtained and stored overnight in the fridge before it was used in the preparation of the printing ink. The printing ink was then prepared by mortar and pestle; first, the dry powders were mixed, and then glycerol, HPMC-gel, and water were added. Upon thoroughly mixing, a brown paste was obtained. The prepared printing ink was transferred into 10 mL Optimum® clear barrel syringes with Optimum® clear pistons (Nordson EFD LLC, Rhode Island, USA) attached with 16 G precision tips (Nordson EFD LLC, USA) and left to stand for 2 h prior to printing. A placebo ink to be used as a reference was prepared in the same manner without the addition of the drug.

3.3. Ink characterization

The prepared drug-loaded ink and the placebo solution were visually inspected, and the viscosity of the formulations was analyzed with a rheometer.

3.3.1. Rheology

Rheology measurements were performed to investigate the viscosity of the printing ink and the placebo solution under the influence of shearing. The measurements were performed at 0, 2, 4, 6, 8, 10, 12, and 24 h after preparation to investigate the viscosity vs. shear rate over time. The measurements were carried out with the HAAKE™ MARS™ Modular Advanced Rheometer system equipped with a plate rotor of 35 mm in diameter (P35/Ti) and a matching lower plate (TMP35), all by Thermo Fischer Scientific (Karlsruhe, Germany). The measuring gap was set to 1 mm and the temperature to 23 °C. Each sample was pre-sheared at a rate of 1 s^{-1} for 30 s, followed by 60 s of equilibration. After that, a shear rate ramp of 0.01–1500 s^{-1} was applied over a running time of 350 s with 5 s per data acquisition point. The manufacturer's software HAAKE™ RheoWin Job Manager v. 4.87.0001 was utilized for test setup and monitoring. The obtained flow curves of viscosity vs. shear rate were analyzed with HAAKE™ RheoWin Data Manager v. 4.87.0001. The printing ink and the placebo solution were measured at least twice, and if differences in the flow curves were observed, a third measurement was performed.

3.4. Computer-aided design

Seven different sizes were designed utilizing a computer-aided design (CAD) software (Autodesk Fusion 360 by Autodesk, 2.0.10446, 2020) in order to investigate the accuracy of the printing technology in the production of tailored gabapentin-containing ChewTs. The seven different designed sizes were named according to the increasing length of the designed rectangles, size 2, 5, 10, 15, 20, 30, and 40, were designed to have the equivalent length in mm, the width and the height were kept constant at 10 and 1 mm respectively.

3.5. Semi-solid extrusion 3D printing

SSE 3D printing is a material extrusion technique that deposits a gel or a paste according to a pre-determined design. The Brinter 1 3D Bio-Printer (Brinter Ltd, Turku, Finland) attached with a Pneuma Tool print head (Brinter Ltd, Turku, Finland) and a compressor was utilized in this study. The Pneuma Tool print head enables low to medium viscosity inks, pastes, or gels to be dispensed with the aid of pressurized air. The pre-loaded syringes attached with 16 G nozzles were placed into the print head prior to printing. In the browser-based Brinter printing software, the print settings were set to 1 mm layer height, 1 shell, and solid fill with a 45-degree fill angle. The print speed was set to 8 mm/s and the pressure to 290 mbar during printing to achieve therapeutic doses between 10 mg and 200 mg. The 3D-printed tablets (printlets) of seven different sizes were printed on transparency poly sheets (Folex imaging X-10.0 copier films, Paper Spectrum Limited, Leicester, UK) placed on top of an analytical balance to achieve accurate doses, and the printlets were left to dry at room temperature for 48 h prior to analysis. The time it took to print 8 squares of size 10 printlets was recorded.

3.6. Characterization of the dosage forms

3.6.1. Physical appearance

The physical appearance of the printlets was visually inspected and photographed. Further, the thickness of the printlets was determined in the middle and all four corners of the dosage form with a caliper (Absolute Digimatic by Mitutoyo Corp, Kawasaki, Japan), and the weight was measured with an analytical balance (Radwag Wagi Elektroniczne by Radwag, Radom, Poland). Finally, average and standard deviations for $n = 5$ printlets of each size were calculated.

3.6.2. Mechanical strength

Sufficient mechanical strength is required to ensure the ability to pack, handle, and administer the dosage form. The hardness of the drug-loaded printlets was determined with a texture analyzer TA.XTplus (Stable Micro Systems, Godalming, UK) and the software Exponent, 2013 v. 6.1.4.0 (Stable Micro Systems, Surrey, UK). The texture analyzer was equipped with a 10 kg load cell, heavy-duty platform, and a 5 mm cylinder probe (SMS P5 probe) (all by Stable Micro Systems, Surrey, UK). The probe was brought down with a speed of 2 mm/s until a trigger force of 0.981 N was achieved, after which the probe continued with a speed of 0.10 mm/s for 1 mm. The software recorded the maximum force (N) at the crushing point. The hardness was measured 48 h after printing on size 10 printlets. Five replicates were measured, and the average values with standard deviations were calculated. The room temperature and relative humidity were monitored during the tests.

3.6.3. Moisture content

The moisture content of the drug-loaded printlets was measured 48 h after printing to ensure complete drying. The moisture content of the dosage form is important, as a too low or too high moisture content may influence the chemical and physical stability of the final printlet. The moisture content of the printlets was measured in triplicate with samples weighing approximately 200 mg each. The measurements were performed with a moisture analyzer (Radwag Mac 50/NH by Radwag, Radom, Poland) which measures the moisture evaporation. The samples were heated up to 120 °C, and the endpoint of the test was an equilibrium where the change in mass was less than 1 mg/min. The weight loss in mass-%, which is equal to the moisture content, was recorded. The average values with standard deviations ($n = 3$) were calculated, and the room temperature and relative humidity were monitored during the tests.

3.6.4. Salivary pH-

The salivary pH of the drug-loaded printlets was measured to ensure neutral pH of the dosage form in order to prevent irritation of the oral mucosa. The pH of the printlets was measured at room temperature with an electronic pH meter (Edge R pH by HANNA Instruments, Inc, Woonsocket, USA). Size 10 printlets ($n = 3$) were placed in glass vials and wetted with 1 mL sterile water. After 30 s, the pH electrode was brought to the water surface, and the readings were recorded after 1 min of equilibration (Sjöholm and Sandler, 2019). The pH values and the temperatures were recorded, and average values with standard deviations were calculated.

3.6.5. Drug content

When determining the suitability of a method for the production of tailored doses at or close to the point-of-care, the ability of the said method to produce dosage forms with an accurate amount of drug is of the highest importance. In this study, the drug content was determined with the ascorbic acid (AA) derivatization method, which was determined by this study to give reliable results when quantifying gabapentin. The general procedure for content measurement consisted of dissolving the printlets in 100 mL purified water in borosilicate flasks. The sealed flasks were fixed in an orbital shaker (Multi-Shaker PSU 20 by BIOSAN, Riga, Latvia) and shaken at 150 rpm for three hours to ensure that the printlets were completely dissolved. Samples of 0.1–0.5 mL were drawn from each solution and derivatized according to the AA method, described by Adam et al. For the method, a 2 mg/mL AA reagent was prepared by adding 200 mg AA, 1 mL purified water, and 20 mL dimethyl sulfoxide (DMSO) to a 100 mL volumetric flask (Adam et al., 2016). The flask was shaken for five minutes and then completed to the mark with DMSO. The aliquots of samples were transferred to Falcon tubes and the volumes were adjusted to 0.5 mL with purified water. 2 mL AA reagent and 7.5 mL DMSO were added, after which the samples were heated on a boiling water bath for 30 minu, cooled down, and spectrophotometrically measured. The absorbances of the drug-loaded samples were measured against samples prepared from the corresponding placebos. Using placebo for blank calibration ensures accurate measurement of the drug's absorbance, as the potential absorbance from the excipients is omitted.

3.6.6. In vitro disintegration

The disintegration time of the printlets was determined with the Sotax DT2 tablet disintegrator (Sotax, Allschwil, Switzerland), which corresponds to apparatus A (basket-rack assembly) described under chapter 2.9.1. in Ph. Eur. 10.0 (Y. European Pharmacopoeia Commission 2020). Ph. Eur. specifies that capsules and film-coated tablets should disintegrate within 30 min, uncoated tablets within 15 min, and orodispersible tablets within 3 min. There is no specification for the disintegration time of a chewable dosage form. FDA recommends that a chewable tablet should disintegrate within the limit for an immediate release tablet (FDA, 2018). The test was carried out in 37 °C purified water in 1-liter beakers. Transparent plastic discs were placed in each tube to prevent the printlets from floating away. The test was performed on size 10 printlets ($n = 6$). The time was recorded until complete disintegration was observed, and the apparatus was operated until all six samples had disintegrated completely.

3.6.7. In vitro dissolution

The dissolution profile was determined for printlets size 10 and for

pure GBP. For dissolution testing of solid oral dosage forms, pH. Eur. assigns the methods described under 2.9.3 (Dissolution test for solid dosage forms) (European Pharmacopoeia Commission 2020). As each sample will have to be treated with the chosen derivatization method before absorbance measurement, the dissolution setup must allow for manual sampling. Furthermore, as each sample is diluted during the derivatization, the dissolution medium's volume must be small to acquire detectable absorbance values. A suitable setup was modified from Apparatus 3 (Reciprocating cylinder).

The test was carried out in the temperature-controlled water bath equipped with a horizontally reciprocating rack to provide a mixing movement, which was set to 50 rpm. The water bath was kept at a temperature of 37 °C. The test was carried out in purified water as the dissolution medium; 100 mL was chosen as a suitable medium volume. The printlets were placed in spiral sinkers to prevent them from floating in the flasks.

Printlets as well as pure GBP were analyzed in triplicate. Since the sampling requires significant manual labor, the time points cannot be as frequent as in automated dissolution setups. Sampling was therefore performed at 1, 5, 15, 30, and 60 min, and after that, with one-hour intervals until the absorbance values reached a plateau. Samples of 0.5 mL were withdrawn at the specified timepoints and replaced with the same amount of 37 °C dissolution medium. The drawn samples were derivatized with the AA method described in 3.6.5. The absorbances of the printlets were adjusted by subtracting the corresponding average placebo absorbance for each timepoint. From the adjusted absorbances, the released drug amount was calculated (taking into account the cumulative amount of drug in the already withdrawn samples). The average percentages of released drug and the standard deviations were calculated for the printlets and pure GBP. The dissolution profiles were plotted as the percentage of the released drug as a function of time.

3.6.8. Solid-state characterization

In the current study, the solid-state of pure gabapentin, the prepared drug-loaded printlet, extruded placebo solution, and physical mixtures were analyzed with Differential Scanning Calorimetry (DSC) and Attenuated Total Reflection-Fourier Transform Infrared Spectroscopy (ATR-FTIR). The physical mixtures were prepared by mixing the raw materials in the same ratios as the prepared solutions. Physical mixture 1 contained gabapentin, HPMC, mannitol, crospovidone, glycerol, and liver powder, and physical mixture 2 was prepared with the same raw materials except for the drug, corresponding to the drug-loaded printlet and placebo extrudate, respectively.

3.6.8.1. Differential scanning calorimetry. DSC analyses were performed with the Q2000 instrument by TA Instruments (New Castle, DE, USA). Data were analyzed with the TA Universal Analysis software v. 4.5A by TA Instruments. Approximately 2 mg of each sample was weighed, placed in Tzero aluminum pans, and sealed with matching Tzero lids (TA instruments, Switzerland). Nitrogen was used as the purge gas with a flow rate of 50 mL/min. A heating ramp was used, measuring the samples from 20 to 200 °C with a heating rate of 10 °C/min. A minimum of two measurements was run for each sample, and if there were any differences observed, a third measurement was performed.

3.6.8.2. Attenuated total reflection-fourier transform infrared spectroscopy. ATR-FTIR spectroscopy measurements were carried out with the UATR-2 Spectrum Two by PerkinElmer (Llantrisant, UK). A force of 75 N was applied to all samples on the crystal. The samples were measured over a range of 4000 to 400 cm^{-1} with 4 accumulations at a resolution of 4 cm^{-1}. Each sample was run twice, and a third measurement was performed if any differences were observed between the first two runs. The spectra were acquired with the PerkinElmer software Spectrum v. 10.03.02 and treated with the program functions baseline correction, normalized ordinate to 3%T, and data tune-up.

4. Results and discussion

4.1. Spectrophotometric quantification

A large part of the study was dedicated to assessing gabapentin quantification methods utilizing UV–Vis spectrophotometry, this was performed in order to facilitate implementation of quality assurance of gabapentin (GBP) at compounding sites. Observations and general discussion on the method's performance is discussed below. For method comparison, the absorbance spectra displaying the absorbance peaks are gathered in section4.1.1. . The results from the method validation are presented and discussed in section 4.1.2., along with figures presenting the plots and regression lines (calibration curves).

The non-derivatization methods were simple and rapid procedures as they did not involve any reaction steps. The MQ method was found to have high precision, consistently giving similar absorbance readings between measurements, and was therefore also tested on GBP-containing dosage forms. However, the low native absorbance of GBP posed problems, and the drug content in the dosage forms could not be reliably quantified. The ET method appeared to give rise to a more unstable state of the GBP molecule as the absorbance peak varied between measurements. In addition, no reliable absorbance readings were obtained in concentrations below 20 μg/mL, hence the method was not further examined.

The condensation product formed between NIN and GBP is a purple complex known as Ruhemann's purple (Abdellatef and Khalil, 2003). The NIN-derivatized samples showed an increasingly intense purple color with increasing GBP concentration. Different heating conditions for the NIN method were investigated, but no correlation was observed. This is supported by the observations of Bali and Gaur, who utilized NIN derivatization on pregabalin and studied the effect of different heating times and temperatures (Bali and Gaur, 2011). The authors concluded that heating the samples for longer than 20 min at 70–75 °C did not produce an improvement in color. Abdellatef and Khalil remark that prolonged heating at higher temperatures weakens the color intensity, so the heating time should be controlled (Abdellatef and Khalil, 2003). It was observed that the NIN-DMF method overall yielded higher color intensity (i.e., higher absorbance values) than NIN-MET. However, both methods expressed highly varying absorbance values between stock solutions and on different days. This finding indicates poor precision and robustness. As expected, adjusting the reaction volumes to equal (variant B) improved the results, especially for the NIN-MET method. The plots were visibly more linear as compared to variant A with unequal reaction volumes. Diluting the samples to 10 mL before heating (variant C) did not work for either method as the reaction medium became too dilute; no complex formation and, therefore, no absorbance readings were obtained in the samples. When testing the NIN method on GBP-containing dosage forms, no visible complex formation or measurable absorbance was obtained in any of the samples, and thus the NIN methods could not be applied to the quantification of GBP in this study.

The AA method is based on the formation of a condensation product between GBP and AA (Adam et al., 2016). An advantage (as compared to NIN derivatization) is the lack of several pipetting steps; all the pipetting was executed at once, after which the samples were heated, cooled down, and measured. The method showed good performance with high precision between assays, and it was found to be both reliable and robust. The quantification range was broad, and samples containing as little as 0.5 and 1 μg/mL GBP were detected and fit the calibration curves. The most linear plots were obtained by keeping the total water volume (stock solution + additional water) of the sample at 0.5 mL and measuring the absorbances at 376 nm. The method was tested several times on the selected GBP dosage form, and the recovered drug content was consistent to the theoretical drug amount.

The VAN method is also based on the formation of a condensation product (Abdellatef and Khalil, 2003). All of the VAN derivatization

methods had to be performed several times to obtain readable absorbance values. Many attempts at calibration curves failed due to the lack of detectable absorbance in the majority of the samples, indicating that a reaction had not occurred. Similarly to the NIN methods, the VAN methods showed high variation in the absorbance values between assays, indicating a lack of precision. The GBP-VAN complex did not yield any visible color. Contrary to the findings of Kazemipour et al., increasing the buffer pH to 8.5 did not increase the absorbance of the GBP-VAN complex (Kazemipour et al., 2013). Instead, the change seemed to yield poorer results with a higher degree of scatter. Given the many required attempts at VAN derivatization, the highly varying results may, unfortunately, be characteristic of VAN methods in general. Both VAN7.5 and VAN8.5 exhibited some linearity in higher concentrations ≥30 μg/mL. The conclusion was made that these methods were

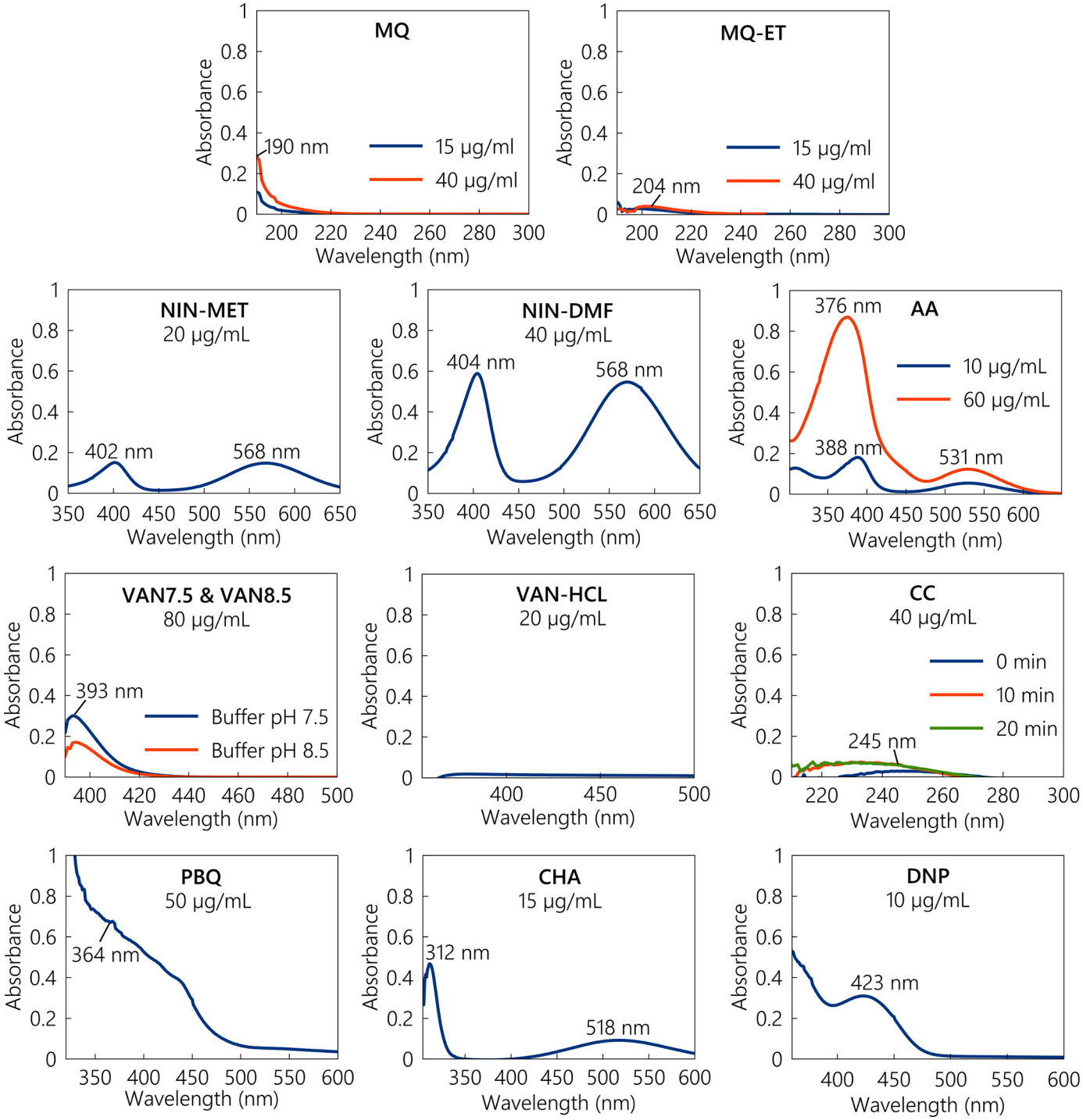

Fig. 1. Absorbance spectra of each gabapentin quantification methods, plotted as absorbance vs. wavelength (nm). The sample concentration on which the scan was performed is given, and the wavelength of each absorbance maximum is defined.
MQ = native absorbance in water; MQ-ET = native absorbance in water/ethanol; NIN-MET = derivatization with ninhydrin in methanol; NIN-DMF = derivatization with ninhydrin in N,N-dimethylformamide; AA = ascorbic acid derivatization, VAN7.5 & VAN8.5 = vanillin derivatization with buffer pH 7.5 or 8.5; VAN—HCl = vanillin derivatization in methanolic HCl; PBQ = p-benzoquinone derivatization; CC = cupric chloride derivatization; CHA = chloranilic acid derivatization; DNP = derivatization with 2,4-dinitrophenol.

not applicable for quantification of GBP due to the unreliable performance. The VAN—HCl method could not successfully be replicated.

The PBQ method, like the AA method, has few working steps as all pipetting is performed before heating. GBP and PBQ formed complexes with an intense reddish-brown color. The color intensity is not attributable to GBP alone, as the drug-free samples used as reference samples also obtained a strong color. The PBQ method showed good precision with similar absorbance readings between assays. In most cases, the method exhibited good specificity. As the PBQ method was found to be relatively reliable, it was also tested on the GBP formulations. However, the PBQ-derivatized drug-loaded samples gave absorbance readings that were too low and, therefore, did not accurately quantify the GBP content. As with NIN derivatization, it is likely that the excipients interfered with the reaction.

For the CC method, different reaction times were investigated, and it was found that increased absorbance readings were obtained when the samples were given time to react. The method was difficult to replicate successfully. It had to be performed several times to obtain absorbance readings in enough samples in order to analyze the results. The GBP-CC complex was seemingly unstable, as the absorbance values varied highly depending on the reaction time. The best results were obtained from a 10 min reaction time, after which a somewhat proportional relationship between absorbance and concentration could be observed in a high concentration range. Due to the unreliable performance and the lack of linearity in relevant concentration ranges, the CC derivatization was not investigated on the GBP dosage forms.

Both the CHA and the DNP methods are electron donor-acceptor reaction with rapid reaction, simple procedure, and development of intensely colored complexes. Both methods suffer from the same limitation regarding the low solubility of GBP in ACN, they both showed a good performance, but were not further investigated since the medium is not relevant for dissolution testing on the dosage forms in this study.

4.1.1. Absorbance spectra

The absorbance spectra displaying the absorbance peaks of each method are presented in **Fig. 1**. For easier comparison of the peaks, the y-axes have been scaled to the same size for all spectra. The absorbance spectra (wavelength scans) were gathered on a sample approximately from the middle of the linear concentration range reported by the respective authors, which explains the varying choices of concentration. It was, however, not possible to choose a concentration from the middle range in all methods. In the case of the MQ, MQ-ET, and VAN—HCl methods, the wavelength scans were performed on chosen concentrations above the reported linear ranges, as the absorbances of the samples within the reported linear ranges were too low to properly detect the absorbance maxima. In some other methods, the reported linear ranges occurred in very high concentrations, and a lower concentration more relevant for the study purposes was chosen.

For the MQ method, the maximum absorbance of GBP in water was found to occur below 190 nm, i.e., outside the instrument's limits. The measurements were carried out at 190 nm, where the absorbance was still relatively high. This finding complies with that of Fonseca et al. (Fonseca et al., 2017). In the MQ-ET method, it was found that the change of solvent shifted the absorbance peak to higher wavelengths, varying between 199 nm and 204 nm, measurements were performed at 204 nm. The found absorbance maxima for both NIN methods correspond to those reported in the original studies (Abdellatef and Khalil, 2003; Galande et al., 2010; Siddiqui et al., 2013). The intensities of the peaks at 402 nm and 404 nm were marginally higher than those at 568 nm and were used for the analysis. For the AA method, a shift in the absorbance peak can be observed when comparing the wavelength scan performed on samples of 10 μg/mL and on 60 μg/mL. The lower peak clearly shifts from ~388 nm to ~376 nm with the increase of the analyte concentration. The wavelengths obtained when measuring the lower concentration corresponds to the ones found in the literature (Adam et al., 2016), but when the whole concentration range was measured at 376 nm (found for the higher analyte concentration), the best linearity was obtained. The VAN7.5, VAN8.5, CC, and DNP methods' absorbance peaks are close to the wavelength peaks reported in their corresponding literatures (Abdulrahman and Basavaiah, 2011; Fonseca et al., 2017; Anis et al., 2011). Minimal absorbance could be observed for the VAN—HCL method around 400 nm, but the intensity was not enough to give a useful absorbance maximum. As is evident in **Fig. 1**, a distinct absorbance peak for the PBQ method was not found. Measurements were carried out at 364 nm, where the absorbance was relatively high. This value is close to the detection wavelength used in the previous studies (Fonseca et al., 2017; Abdellatef and Khalil, 2003). Absorbance maxima for the CHA method were found at 312 nm and 518 nm, of which the former had a considerably higher intensity. Siddiqui et al. utilized the same absorbance peak, which in their measurements was found at 314 nm (Siddiqui et al., 2010). Salem carried out the measurements at 535 nm (Salem, 2008).

4.1.2. Method validation

For each assay, method validation was performed. The absorbance values were plotted as a function of the GBP concentration. The linearity of the plots was visually evaluated, and lines were fitted with linear least squares regression to obtain calibration curves. When plotting the data, a few obvious outliers were visually identified and discarded. The outliers were due to unknown errors in sample preparation or measurement. In practice, this comprised values that were incoherent or absurd, such as negative absorbance values. Some methods consistently exhibited varying and non-proportional absorbances in the lower concentration ranges; these values were included in the plots to illustrate the characteristics of the method. In some methods, the plot could be split into two separate linear ranges.

In general, a linear calibration curve should have a slope statistically significant from zero to ensure the sensitivity of the method and that the absorbance increases proportionally with increasing analyte concentration. To ensure specificity, the (y-)intercept should not be statistically significant from zero – if the analyte concentration in the sample is zero, the absorbance should ideally be negligible. The coefficient of determination (R^2) is often used as a measurement of linearity, but it should not be trusted as the only tool for linearity assessment. A perfectly linear relationship yields an R^2 value of 1; thus, an R^2 close to 1 is considered an attribute of a good quality calibration curve. However, R^2 can return seemingly good values, for instance, if the plot is curve-shaped or the data points are symmetrically scattered around the regression line. Therefore, it is equally important to visually inspect the data points. Investigating the residual sum of squares (RSS) can be useful in evaluating the quality of a calibration curve (Moosavi and Ghassabian, 2018). The RSS comes from the sum of all the squared deviations from the fitted line – in other words, the RSS is a tool for expressing the degree of scatter and how well the values fit the model (the regression line). A small RSS indicates a tight fit of the data points to the model.

The results from the regression analysis are presented in **Table 2**, in which the most relevant parameters have been included. Comparing the RSS values was found not to give much valuable information in this method assessment; the RSS values were overall very low (all except one were <0.005), and the values did not predict the quality of the calibration curves or usefulness of the methods, and therefore, the information was excluded from the table.

As can be observed from **Table 2**, the R^2 values were reasonably high for all methods. In most cases, however, the R^2 did not describe the true linearity very well on its own. This is, in fact, accurate for all statistical parameters if they were to be examined individually; thus, when interpreting the regression analysis and validating quantification methods, several parameters must be assessed. Visual evaluation of the scatter and the goodness of fit is also important. A high slope, which generally indicates good sensitivity, was not always equal to a good quality calibration curve; the lines with a relatively high slope also exhibited a y-intercept different from zero, or an R^2 below the preferred minimum of

Table 2
A table with all the tested quantification methods and its relevant analytical parameters.

Method	Tested concentration range (μg/mL)	Linear concentration range (μg/mL)	λ_{max} (nm)	Slope	Intercept	R^2
MQ	0.25–80	5–80	190	0.0079	−0.0171	0.9997*
MQ-ET	0.5–80	20–80	204	0.0007	0.0052*	0.9829
NIN-MET						
A	1–80	10–70	402	0.0035	0.1674	0.9627
B	1–80	5–80	"	0.0069	−0.0053*	0.9922
C	5–150	N/A	N/A			
NIN-DMF						
A	1–80	5–30	404	0.0221*	−0.0823	0.9945
B	1–80	30–80	"	0.0348*	−0.4116	0.9946
C	5–150	1–20	"	0.0042	−0.0030*	0.9778
		30–80	"	0.0120*	−0.2459	0.9898
		70–130	"	0.0008	−0.0178	0.9907
AA	0.5–80	0.5–40	376	0.0158*	−0.0023*	0.9998*
		40–80	"	0.0118*	0.1594	0.9972
VAN7.5	1–140	30–120	393	0.0019	0.0283	0.9949
VAN8.5	1–140	40–140	394	0.0020	−0.0304	0.9729
VAN-HCl	1–20	N/A	N/A			
PBQ	1–180	2.5–60	364	0.0120*	0.1134	0.9924
		60–140	"	0.0079	0.3669	0.9933
CC	0.5–140	60–120	244	0.0019	0.0513	0.9904
CHA	1–80	1–60	312	0.0159*	0.0132	0.9993*
DNP	1–80	1–10	423	0.0400*	0.0496	0.9981
		15–70	"	0.0115*	0.3275	0.9927

MQ and MQ-ET = native absorbance of gabapentin in water or water/ethanol. NIN-MET and NIN-DMF = derivatization with ninhydrin in methanol or N,N-dimethylformamide. Variants A, B, and C stand for different reaction volumes (see 4.2.4.6.) AA = ascorbic acid derivatization; VAN7.5 and VAN8.5 = vanillin derivatization with buffer pH 7.5 or 8.5; VAN—HCl = vanillin derivatization in methanolic HCl; PBQ = p-benzoquinone derivatization; CC = cupric chloride derivatization; CHA = chloranilic acid derivatization; DNP = derivatization with 2,4-dinitrophenol. Values marked with a * are considered acceptable.

0.999.

An interesting observation was that in many methods, the results were affected by the concentration of the stock solutions. This was observed as variations in the linearity and the precision of the absorbance readings. All methods were tested on at least two different gabapentin stock concentrations, and differences were noticed in all methods except for the AA method. In many methods, the absorbance values for a specific concentration showed variations greater than 0.1 absorbance units between batches. In theory, different stock concentrations should not affect the results, as the molar proportions in the reactions remain the same (assuming that the solvent proportions are not changed). This variation can indicate decreased robustness and precision of a method.

The calibration curves corresponding to the regression analysis results are presented in Fig. 2. All other methods could be performed throughout the whole analyzed concentration range with the same stock solution, but for the AA method, two separate stock solutions had to be utilized. Since the total water volume of each sample was adjusted to 0.5 mL, the samples with higher GBP concentration required the use of a stronger stock solution in order not to exceed the defined water volume. A stock solution of 1 mg/mL was utilized for the concentration range 0.5–40 μg/mL, and respectively, 2 mg/mL for the range 40–80 μg/mL.

The AA method exhibited the best performance throughout each assay. The method performed well in the method validation, returning the highest R^2 and the intercept closest to zero, and was the only method that yielded good values for all three inspected analytical parameters (marked with a * in Table 2). Furthermore, linearity ($R^2 = 0.9998$) was achieved in relevant concentration ranges, making the method applicable to dissolution testing of the small-dose formulation in this study. Of the methods which were tested for determining the drug content in dosage forms, the AA method was the only precise and reliable method. Thus, a quantification method that fulfilled the study aims had been found, and the study could proceed with the proof-of-concept part consisting of dosage form manufacturing and analysis.

4.2. Ink characterization

The drug-loaded ink and the placebo solution were visually characterized to ensure homogeneity. Both formulations had a brown color and a scent of liver powder due to the addition of liver powder as a taste-enhancing agent. The obtained drug-loaded ink was a thick bubble-free paste suitable for 3D printing. The placebo solution had a lower viscosity than the drug-loaded ink and did thus not keep shape upon extruding.

4.2.1. Rheology

The rheological behavior of the drug-loaded printing ink and the placebo solution was examined by measuring the change in viscosity as a function of increasing shear rate at 0, 2, 4, 6, 8, 10, 12, and 24 h after preparation. The viscosity curves are pictured in Fig. 3. As can be seen in the curves, the solutions exhibited non-Newtonian fluid behavior with shear-thinning properties. The difference in viscosity that was noticed between the formulations was affirmed with the rheological analysis. The placebo solution exhibited a lower viscosity compared to the drug-loaded ink. This is due to the increased solid fraction of the drug-loaded ink with the addition of gabapentin, which leads to an increase in viscosity. To decrease the risk that change in viscosity over time might pose on the printing result, the 2–12 h window after ink preparation was chosen as the printing window for this study.

4.3. Semi-solid extrusion 3D printing

The Brinter printer was successfully utilized in the production of gabapentin-containing printlets for the treatment of veterinary patients. The drug-loaded ink was printable, and the designed seven different sizes were printed with a wet weight correlating in accordance with escalating size ($R^2 = 0.9958$). In order to achieve a therapeutic dose range of 10–200 mg in the lowest possible amount of time, the optimal print settings were found to be 1 print layer with a layer height of 1 mm, 1 shell, and a solid infill with a 45-degree angle. A print speed of 8 mm/s was found appropriate in combination with a pressure of 290 mbar. The time it took to print 8 printlets of size 10 was on average 2 min and 12 s. In order to decrease the print time, the print speed could further be increased. If the print speed is increased, the pressure has to be increased as well to obtain the same amount of material during faster printing. The viscosity of the placebo ink was too low to be printed with a 16 G tip, and

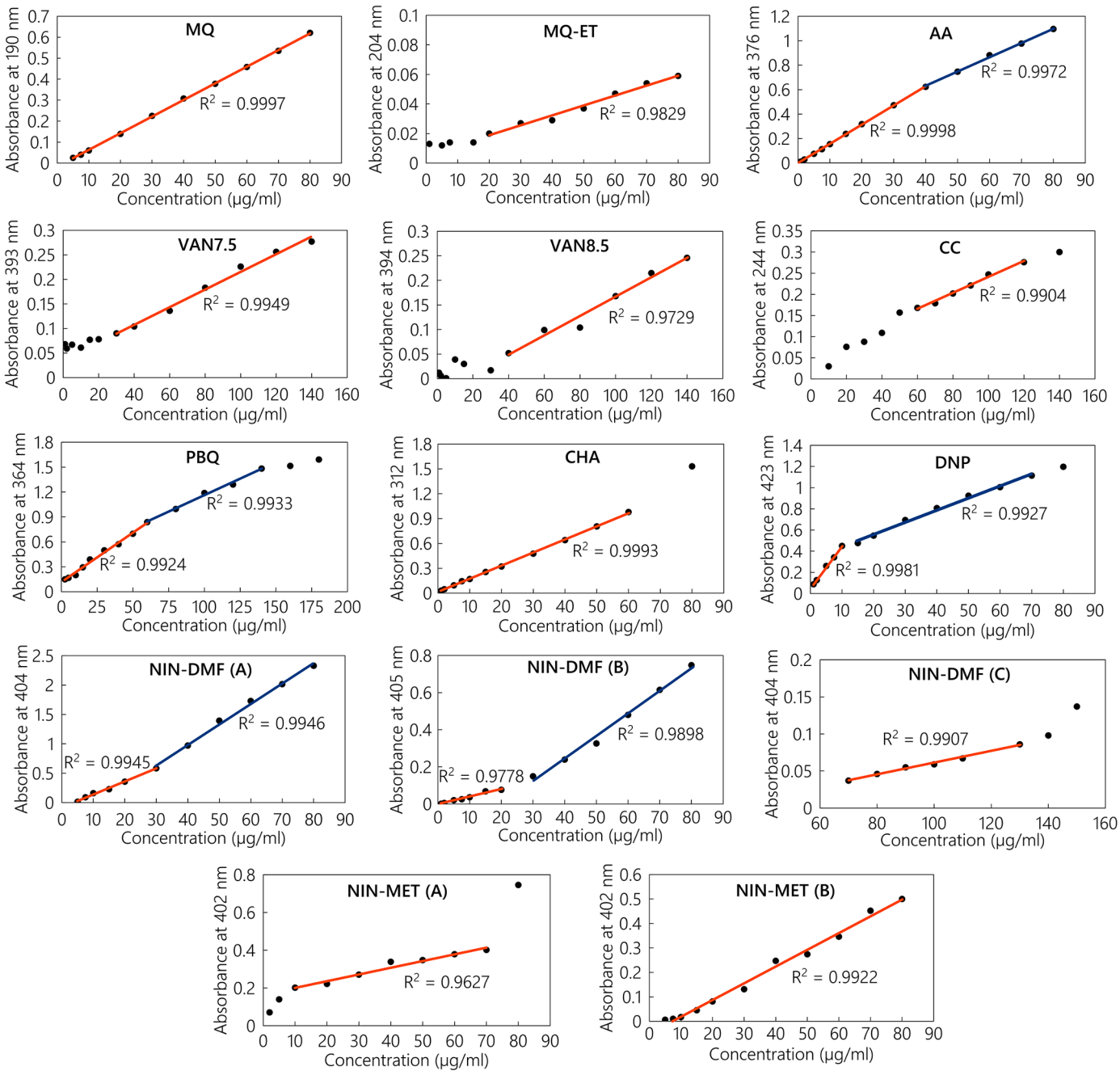

Fig. 2. The absorbance-concentration plots for the assessed methods, with calibration curves showing the linear ranges.

the decision was made to manually extrude the placebo solution to be used as a reference for drug content determination and dissolution testing.

4.4. Physical appearance

As mentioned, the average wet weight of the printlets had a great correlation with the designed size. As expected, a high correlation between size and dry weight ($R^2 = 0.9966$) and between wet weight and dry weight ($R^2 = 0.9998$) was obtained. This indicates that SSE 3D printing is suitable method for the preparation of tailored dosage forms. The thickness of the printlets increased with increasing size, from an average thickness of 1.17 mm to 1.97 mm, due to surface tension-dominating behavior. As can be seen in Fig. 4, the printed dosage forms are rectangularly shaped (with rounded corners due to the surface tension-dominated behavior) with a brown color and an escalating size in correspondence with the CAD. As animals dislike too chewy dosage forms (Aleo et al., 2018), the prepared hard ChewTs in this study, with a brown color and an apparent liver scent, resembling a dog or a cat treat, are expected to have a high voluntary acceptance which is the cornerstone of success in the medicinal treatment of animals.

4.5. Mechanical strength

The mechanical strength of the dosage form was determined to ensure sufficient hardness for packing, handling, and administrating the dosage form. The hardness of a ChewT is generally lower than that of conventional tablets to enable chewing of the dosage form. The satisfactory hardness of uncoated tablets is considered to be 30–50 N/cm^2 (Arora et al., 2013). The results obtained from the measurement were

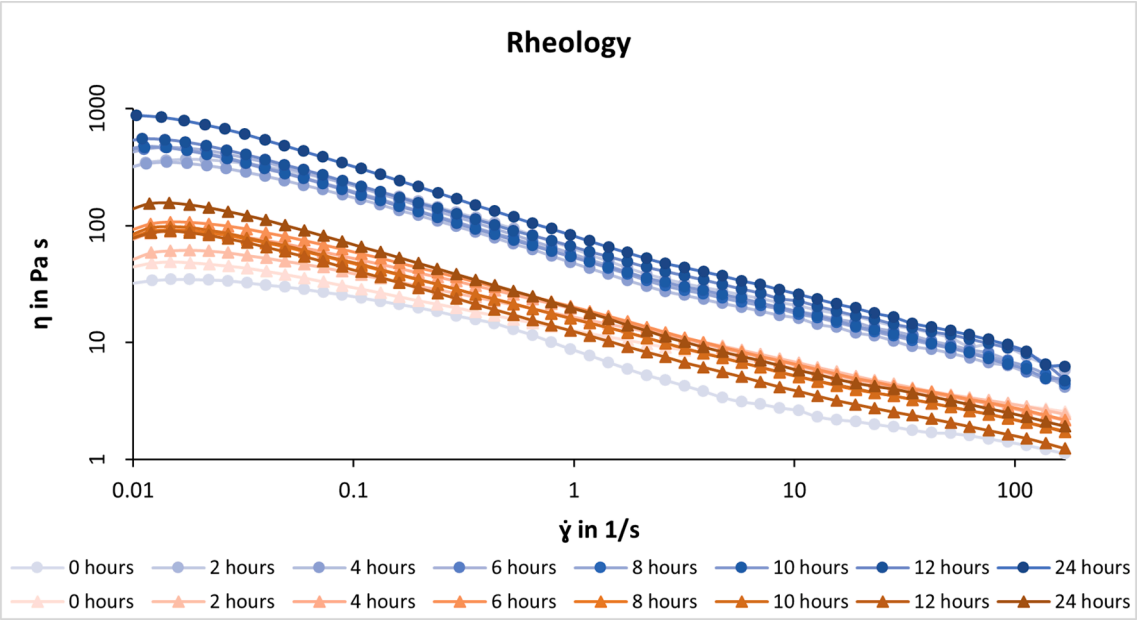

Fig. 3. Viscosity vs. shear rate curves measured at 0, 2, 4, 6, 8, 10, 12, and 24 h after preparation. Placebo solutions are visualized in orange colors with triangular markers and drug-loaded inks are visualized in blue colors with round markers.

Fig. 4. Photographic image of the semi-solid extrusion 3D-printed gabapentin-containing chewable tablets of different doses.

9.24±0.61 N/19.63mm^2 equaling 47.07±3.11 N/cm^2, which is right in line with the proposed strength. FDA recommends a chewable tablet having a hardness of less than 12 kp (FDA, 2018), this corresponds to 118 N. The prepared ChewTs in this study obtained a hardness below this threshold, making them suitable to be used as chewable dosage forms. The measurements were performed on size 10 printlets at 21.5 ± 0.1 °C and 35.5 ± 0.1% RH.

4.6. Moisture content

Low moisture content can be crucial for the stability of a dosage form, but a too low moisture content can yield brittle tablets. There is no set limit for the preferred moisture content for ChewTs. In this study, the moisture content of the dried printlets was found to be 3.7 ± 0.6%M, measured at ambient conditions (20.9 ± 0.0 °C and 35.0 ± 0.3% RH).

4.7. Salivary pH

The salivary pH of the dosage form was investigated, as administering a chewable dosage form with a too acidic or basic pH value can cause irritation and damage to the oral mucosa (Nair et al., 2013). Ideally, the pH of chewable dosage forms should be neutral, close to 7. The obtained average pH value ($n = 3$) of the prepared ChewTs was 7.0 ± 0.4. The found pH of the dosage form was ideal for oral administration and should not cause any discomfort to the patient upon administration.

4.8. Drug content

In order to assess a techniques suitability to be used for compounding of tailored doses, therapeutic doses need to be obtained as well as a high correlation between the designed and the obtained dose. The average weights of the dry, prepared printlets ranged between 87.8–500.0 mg for the different sizes with a high correlation ($R^2 = 0.996$) between the designed size and dry weight of the dosage form. The obtained drug amount reached from around 10 mg for the smallest printlet to over 200 mg for the biggest printlet, with a correlation of $R^2 = 0.9935$ between designed size and drug amount. The obtained results show that therapeutic doses can be obtained utilizing SSE 3D printing. The current problem of the marketed GBP products is that the doses are too high for treating small cats and dogs, hence compounding of small doses is of high priority. In this study we obtained doses as small as 10 mg which are therapeutically appropriate for small dogs and cats and hence this technique is suitable for tackling the current issue. High correlation and good content uniformity, with the highest variation from average being less than or equal to 10%, further indicates this technique as a suitable candidate for compounding tailored veterinary dosage forms at a pharmacy or an animal clinic.

4.9. In vitro disintegration

The disintegration time of the printlets ($n = 6$) in purified water was investigated with a tablet disintegrator. The average disintegration time of the prepared printlets was 3 min and 22 s with an average standard deviation of 34 s. The dosage form complies with the FDA guideline of disintegrating within the timeframe of an immediate release dosage form. It is important that a chewable dosage form exhibits rapid disintegration in order to prevent obstruction of the gastrointestinal tract in the event of the ChewT not being completely chewed by the animal (FDA, 2018).

4.10. In vitro dissolution

Dissolution profiles were determined for the drug-loaded printlet and for pure GBP. The cumulative drug release was plotted as a function of time (Fig. 5). As GBP is freely soluble, 100% drug release is obtained within minutes from pure GBP. The drug release from the printlets is slightly slower, but as expected from the obtained disintegration results, it is still rapid, and more than 90% of the drug was released within 15 min. There is no specific dissolution time requirements for ChewTs, but according to the FDA, ChewTs should meet the same dissolution specifications as immediate release tablets (FDA, 2018), which is 80% drug release within 30 min (U.S. Department of Health and Human Services Food and Drug Administration Center for Drug Evaluation and Reseach 2018). The prepared ChewTs met the said specification. An automated test setup that allows for an increased number of sampling time points would yield a more accurate dissolution profile. Unfortunately, the dissolution must be performed manually as every sample requires a derivatization step in order to calculate the released drug amount.

4.11. Differential scanning calorimetry

The DSC curves are presented in Fig. 6. The evaporation of water around 100 °C was present but only marginally noticeable in most samples. A melting point with a peak onset between 152 °C and 155 °C is observed in both physical mixtures, the placebo, and the drug-loaded printlets. This might be due to shifted melting peak of mannitol in the formulation which has a pure endopeak at 168.4 °C (Jaipal et al., 2015). The onset of the melting point at 167 °C was evident for pure GBP, which complies with literature values (Williams, 2013). A slight small peak can also be found for the drug-loaded printlet with an onset at 168 °C, confirming that the observed crystals in the dosage form are crystallized GBP. A concern when manufacturing GBP dosage forms, is the degradation of GBP to gabapentin lactam. This degradation product should display a distinct melting point around 87–91 °C (Braga et al., 2008; Cutrignelli et al., 2007). This cannot be found in the printlets, which indicates that the GBP has not degraded into gabapentin lactam during the manufacturing process.

4.12. Attenuated total reflection-fourier transform infrared spectroscopy

Attenuated total reflectance-Fourier transform infrared spectroscopy (ATR-FTIR) was utilized to study the solid-state characteristics of the prepared printlet. The FTIR spectra with baseline correction, normalization, and data tune-up adjustments are presented in Fig. 7. GBP is known to exhibit polymorphism; in the solid-state, zwitterionic GBP can form four different polymorphs, of which form II is the commercially used drug substance (Zong et al., 2011). Peaks in the typical NH stretching region (3500–3300 cm^{-1}) would indicate the presence of unionized amine groups, whereas the absence of these peaks confirms the existence of GBP in the zwitterionic state (Lin et al., 2010). The stretching vibrations of the ionized groups (NH^{3+}) are typically noticeable in the 3200–2800 cm^{-1} range (Siddiqui et al., 2010; Ranjous and Hsian, 2013); in Fig. 7, they can be seen as a doublet at 2920 and 2857 cm^{-1} in the pure GBP sample. Siddiqui et al. observed the carbonyl stretch at 1615 cm^{-1}, which corresponds to the observed peak at 1610 cm^{-1} in the pure GBP sample in Fig. 7 (Siddiqui et al., 2010). The found peaks in the pure GBP sample are in line with the peaks characteristic for polymorph II (Lin et al., 2010; Ranjous and Hsian, 2013). The most distinct of these peaks are labeled in the spectrum for pure GBP. Some of the characteristic peaks of gabapentin are hidden by the additives in the spectra obtained of the drug-loaded printlet and physical mixture, but peaks 1534, 1396, and 1165 cm^{-1} can be found and are marked as bold in the figure, indicating that GBP is found in form II also in the prepared dosage form. No difference can be seen between the final dosage form and the drug-loaded physical mixture. The characteristic peaks of the degradation product, gabapentin lactam, have been found to occur around 3202, 2928, and 1699 cm^{-1} (Ranjous and Hsian, 2013). The additives in the formulation have strong peaks in these regions, but no changes in the spectra of the drug-loaded printlets at these wavelengths were observed, confirming the conclusions drawn from the DSC that the manufacturing process did not degrade the drug.

5. Conclusions

The present study aimed to investigate ultraviolet-visible (UV–Vis) spectrophotometric quantification methods in order to quantify gabapentin (GBP) in semi-solid extrusion (SSE) 3D-printed veterinary dosage forms. There are known challenges with quantifying GBP, and the question of interest in this study was whether an easy, rapid, and reliable quantification method could be applied to small-dose veterinary formulations. There is a dire need for the use of new technology for the production of veterinary GBP dosage forms at or close to the point-of-

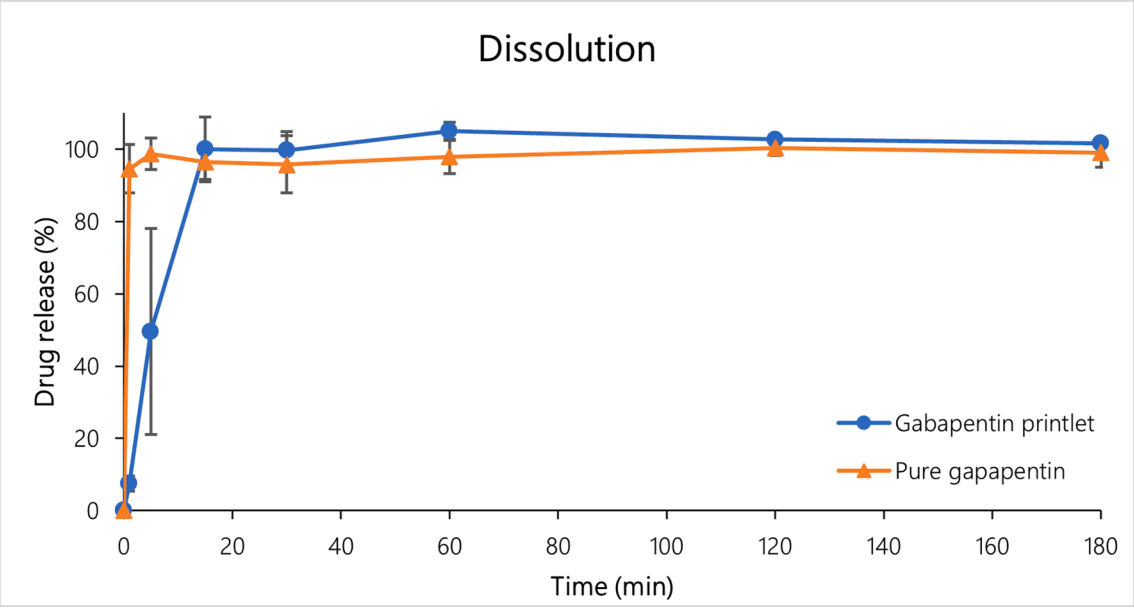

Fig. 5. Drug release dissolution profiles of pure gabapentin and gabapentin printlets in purified water.

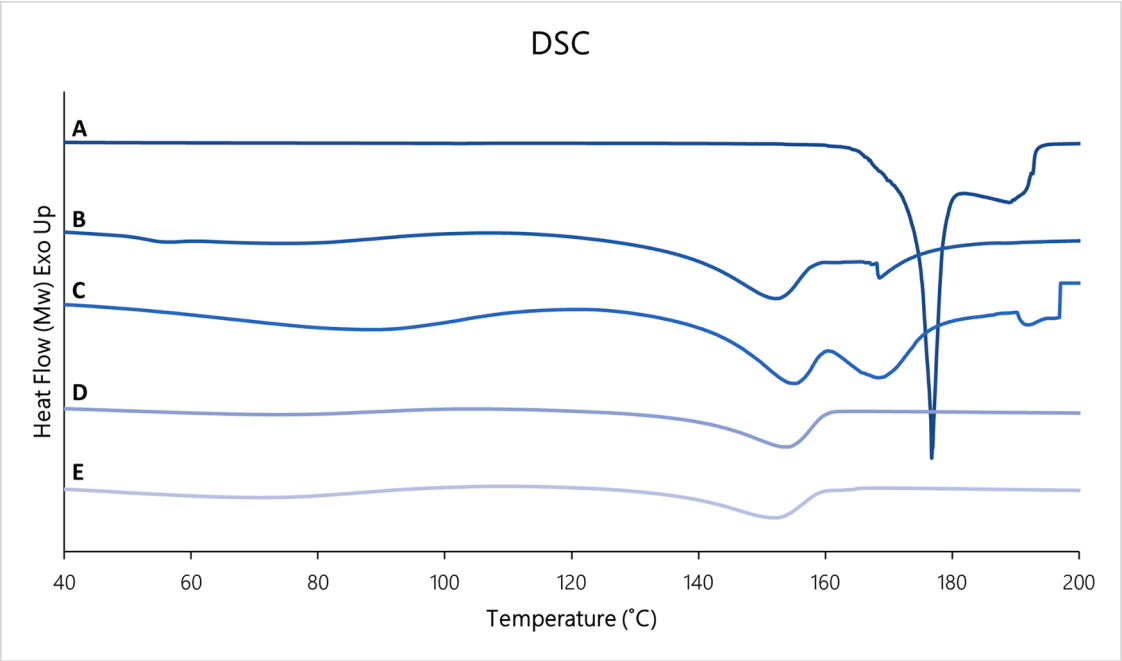

Fig. 6. DSC endothermic curves of A) pure gabapentin, B) drug-loaded printlet, C) physical mixture 1, D) placebo extrudate, and E) physical mixture 2. Physical mixture 1 corresponds to the drug-loaded printlet and physical mixture 2 corresponds to the placebo extrudate.

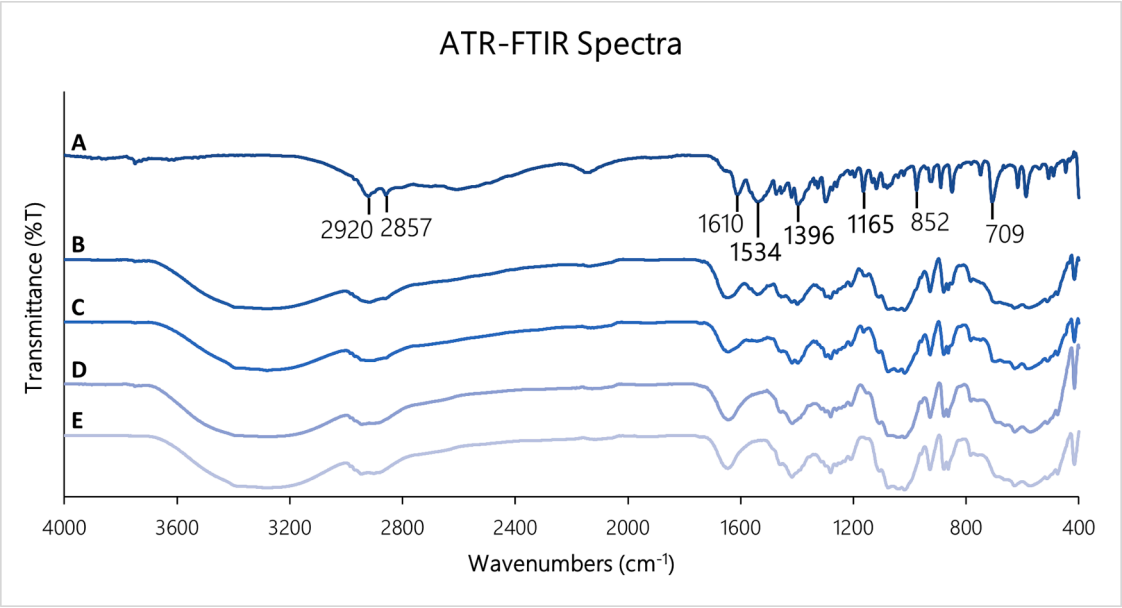

Fig. 7. ATR-FTIR spectra of A) pure gabapentin, B) drug-loaded printlet, C) physical mixture 1, D) placebo extrudate, and E) physical mixture 2. Physical mixture 1 corresponds to the drug-loaded printlet and physical mixture 2 corresponds to the placebo extrudate.

care, but the quantification challenges have been a hurdle in their development. To the best of the author's knowledge, GBP quantification methods have previously not been assessed for the purpose of veterinary medicine, nor have chewable gabapentin dosage forms been prepared by means of printing technologies.

A selection of quantification methods was assessed, and the methods exhibited highly varying performance. One method based on derivatizing GBP with ascorbic acid (AA) exhibited superior performance and was successfully applied to the quantification of GBP in the developed formulation. As a proof-of-concept, the AA derivatization method was applied for determining the content uniformity and the in vitro dissolution profile of the developed dosage forms. Furthermore, the quality of the chewable tablets was assessed through various analysis methods.

The findings proved that GBP could be reliably quantified with the AA derivatization method, both in bulk and in the formulation. As of current, there is a lack of quality control of compounded doses. The use of the AA method described in this article provides an easy and robust mean of quantifying GBP in compounded doses at the compounding site, not only for veterinary dosage forms, but for human medicinal product as well. The developed formulation in this study exhibited good mechanical strength, low moisture content, rapid drug release, and easily adjustable doses to tailor the treatment for each patient's needs. Furthermore, the dosage form exhibited neutral pH and animal appropriate palatability-enhancing characteristics, making it suitable as a

chewable veterinary formulation. These findings are important as there are no commercially available veterinary dosage forms of GBP, and there is a significant unmet need within GBP treatment of small pets.

The findings in this study carry many practical benefits, as they demonstrate that pet-friendly GBP dosage forms can easily be manufactured and analyzed. The UV–Vis quantification method with AA derivatization is simple and can fairly easily be implemented in pharmacies, veterinary clinics, animal hospitals, and such. The suggested chewable formulation of GBP serves as an example of a dosage form that is simple to prepare and enables tailoring of the dose. Implementing these findings in practice could diminish the current need for extensive manual labor when compounding GBP or other drug-loaded dosage forms or the risk associated with the splitting of tablets and capsules. Instead, safe and effective veterinary medicines could be rapidly manufactured at or close to the point-of-care.

Funding

The funding sources had no involvement in the study design, in the collection, analysis, and interpretation of data, in the report's writing, or in the decision to submit the article for publication.

CRediT authorship contribution statement

Erica Sjöholm: Conceptualization, Methodology, Investigation, Writing – original draft, Visualization, Project administration, Funding acquisition. **Rathna Mathiyalagan:** Methodology, Investigation, Writing – review & editing. **Lisa Lindfors:** Conceptualization, Methodology, Investigation, Writing – original draft, Visualization. **Xiaoju Wang:** Methodology, Investigation, Writing – review & editing. **Samuli Ojala:** Conceptualization. **Niklas Sandler:** Conceptualization, Funding acquisition.

Declaration of Competing Interest

The authors declare that they have no known competing financial interests or personal relationships thatcould have appeared to influence the work reported in this paper.

Acknowledgments

We thankfully acknowledge Turku University of Applied Sciences for the use of the Brinter printer. We kindly thank Curify OY for donating gabapentin, Dow Chemical Company for providing Methocel K3 Premium, and BASF for supplying Kollidon CL for the present study.

Funding

This research was funded by the Väisälä Fund through the Finnish Academy of Science and Letters (a personal grant for Erica Sjöholm) and the Finnish Foundation of Veterinary Research (a personal grant for Rathna Mathiyalagan).

Appendix I

Spectrophotometric quantification of gabapentin

Non-derivatization methods

Two non-derivatization methods were performed, one where GBP was dissolved in purified water (MQ) and another where GBP was dissolved in a 1:1 mixture of MQ and ethanol (ET), and the native absorbance of GBP was directly measured. The MQ method has been described by Gujral et al. and Fonseca et al., and the MQ-ET method by Fonseca et al. as well as by Chandra Dinda et al. (Fonseca et al., 2017; Gujral et al., 2009; Chandra Dinda et al., 2012). The methods were implemented by preparing stock solutions of GBP in purified water, or the water/ethanol mixture, from which a range of dilutions was made and measured directly with the spectrophotometer.

Ninhydrin derivatization

Apart from the choice of solvent, the main difference between the published ninhydrin (NIN) derivatization methods is whether the samples are diluted with water to 10 mL before or after heating them. The variant where samples were diluted after heating was labeled A. In the published studies, the reaction volumes in the samples had not been adjusted to equal levels before heating. Since unequal proportions of reagent to reaction volume can potentially affect the accuracy and comparability of the results, a variant B was introduced, where all samples were adjusted to the same (smallest possible) volume before they were heated. The samples were then diluted to 10 mL after heating. In variant C, samples were diluted to 10 mL before heating.

For the NIN-MET method (Siddiqui et al., 2013), a reagent with 2 mg/mL NIN in methanol (MET) was prepared, and the flask was covered with aluminum foil to protect it from light. Aliquots of GBP stock solution in water were transferred to Falcon tubes, and 2 mL NIN reagent was added. For variant A, nothing was further added to the samples before heating; for variant B, purified water was added to adjust the volume of all samples to 3 mL; and for variant C, purified water was added to a total volume of 10 mL prior to heating. The samples were heated in the water bath (protected from light) and cooled down in an ice bath, after which variant A and B samples were diluted to a total volume of 10 mL with water. After heating, cooling down, and dilution, the samples were measured. Different heating conditions have been described in the literature, ranging between 70 °C for 20–80 min and 90 °C for 5 min. In this study, various conditions were tested: 70 °C for 80 min, 70 °C for 20 min, 80 °C for 10 min, and 90 °C for 5 min.

For the NIN-DMF method (Abdellatef and Khalil, 2003; Galande et al., 2010), a reagent with 2 mg/mL NIN in dimethylformamide (DMF) was prepared and protected from light. The method was performed in the same way as the NIN-MET method.

In a study published by Goswami and Jiang, a method corresponding to NIN-MET was utilized to quantify GBP in the aquatic environment (Goswami and Jiang, 2018). The authors describe adding 1 mL of 0.005 M sodium hydroxide to each sample, which is supposed to aid the complex formation between NIN and GBP. The samples were diluted to 10 mL after heating. Although this method was not developed for GBP quantification in bulk or dosage forms, the method was investigated in this study to examine the effect of sodium hydroxide addition on the NIN-MET variants.

Ascorbic acid derivatization

For the ascorbic acid (AA) method described by Adam et al., a 2 mg/mL AA reagent was prepared by adding 200 mg AA, 1 mL purified water, and 20 mL dimethyl sulfoxide (DMSO) to a 100 mL volumetric flask (Adam et al., 2016). The flask was shaken for five minutes and then completed to the mark with DMSO. The samples were prepared by transferring aliquots of GBP stock solution in water to Falcon tubes and adjusting the volumes to 0.5 mL with purified water. 2 mL AA reagent and 7.5 mL DMSO were added, after which the samples were heated on a boiling water bath for 30 min, cooled down, and spectrophotometrically measured.

Vanillin derivatization

Derivatization of GBP with vanillin (VAN) has been performed on GBP stock solutions in water (Fonseca et al., 2017; Abdellatef and Khalil, 2003; Kazemipour et al., 2013). The methods require a Duquenois reagent of vanillin and a McIlvaine buffer with pH 7.5. Kazemipour et al. claimed that increasing the buffer pH to 8.5 would optimize the

reaction yield., i.e., increase the absorbance intensity (Kazemipour et al., 2013). The vanillin methods were therefore tested with a buffer pH of 7.5 (VAN7.5) and a buffer pH of 8.5 (VAN8.5). For comparison, an additional vanillin derivatization method described by Mohammed and Mohamed was tested, namely, the VAN—HCl method (Mohammed and Mohamed, 2015). In this method, both GBP and vanillin solutions were prepared in 1 M methanolic hydrochloric acid.

For methods VAN7.5 and VAN8.5, the Duquenois reagent was prepared by mixing 2 g vanillin with 0.3 mL acetaldehyde and adding ethanol ad 50 mL. The flask was wrapped in aluminum foil to protect the reagent from light. The McIlvaine buffer was prepared by mixing 35.5 mL of a 0.2 M aqueous solution of disodium hydrogen phosphate with 64.5 mL of a 0.1 M aqueous solution of citric acid. The pH was measured with an electronic pH meter (edge® meter equipped with an electrode and software v. 1.08, all by Hanna Instruments, Woonsocket, USA). The pH was adjusted to either 7.5 or 8.5 with 0.1 M sodium hydroxide in an aqueous solution. The method was performed by transferring aliquots of the stock solution to Falcon tubes and adding 1 mL of reagent and 1 mL of buffer. The samples were protected from light and left to rest for 30 min, after which they were completed to 10 mL with purified water and measured.

For the VAN—HCl method, a reagent was prepared by dissolving 5 g vanillin into 100 mL of 1 M methanolic hydrochloric acid. The GBP stock solution was prepared in methanolic hydrochloric acid as well. The samples were prepared by transferring aliquots of the stock solution into Falcon tubes and adjusting the volume to 1 mL with methanolic hydrochloric acid. After that, 2 mL of vanillin reagent was added, and the solutions were set aside for 15 min, after which they were measured.

p-Benzoquinone derivatization

Derivatization with p-benzoquinone (PBQ method) has been described by Abdellatef and Khalil and assessed by Fonseca et al. in their method comparison study (Fonseca et al., 2017; Abdellatef and Khalil, 2003). The method was carried out on GBP stock solutions in water. A PBQ reagent was prepared by dissolving the appropriate amount of p-benzoquinone into ethanol to obtain a concentration of 1 M. Furthermore, a 1 M phosphate buffer was prepared, and the pH was adjusted to 7.5 with sodium hydroxide in an aqueous solution. The method was performed by transferring aliquots of GBP stock solution into Falcon tubes and adding 0.5 mL phosphate buffer and 0.2 mL PBQ reagent. The volumes were completed to 10 mL with purified water, and the samples were heated on a 90 °C water bath for 5 min. The samples were measured after cooling down.

Cupric chloride derivatization

The cupric chloride/copper(II) chloride (CC) method by Anis et al. was carried out on GBP stock solutions in water (Anis et al., 2011). A 0.1% CC reagent in purified water was prepared. A borate buffer was obtained by dissolving 2.5 g sodium chloride, 2.85 g disodium tetraborate decahydrate (Borax), and 10.5 g boric acid per 1000 mL purified water. The pH was adjusted to 7.5 with sodium hydroxide in an aqueous solution. Aliquots of GBP stock solution were transferred into Falcon tubes, and 1 mL of borate buffer was added. The samples were mixed, and then 2 mL of CC reagent was added. The volume was made up to 10 mL with purified water prior to sample measurement.

Chloranilic acid derivatization

Derivatization with chloranilic acid (CHA) has been described by Salem as well as Siddiqui et al. (Siddiqui et al., 2010; Salem, 2008). The method has been developed for GBP stock solutions in acetonitrile (ACN). The CHA reagent was prepared as 1 mg/mL in ACN. The method was executed by first transferring 1 mL CHA reagent into Falcon tubes and then adding the aliquots of GBP stock solution. The volumes were completed to 10 mL with ACN, and the samples were immediately measured.

2,4-dinitrophenol derivatization

Abdulrahman and Basavaiah have developed a 2,4-dinitrophenol (DNP) derivatization method (DNP method) (Abdulrahman and Basavaiah, 2011). Like the CHA method, it also requires ACN as the solvent for GBP. For performing the method, a 2 mg/mL DNP reagent was prepared in dichloromethane. Aliquots of GBP stock solution were transferred into Falcon tubes, 1.5 mL DNP reagent was added, and the samples were diluted to 10 mL with ACN. The samples were mixed, covered with aluminum foil, and left to rest for 10 min before measuring.

References

Abdellatef, H.E., Khalil, H.M., 2003. Colorimetric determination of gabapentin in pharmaceutical formulation. J. Pharm. Biomed. Anal. 31, 209–214. https://doi.org/10.1016/S0731-7085(02)00572-1.

Abdulrahman, S.A.M., Basavaiah, K., 2011a. Sensitive and Selective Spectrophotometric Determination of Gabapentin in Capsules Using Two Nitrophenols as Chromogenic Agents. Int. J. Anal. Chem. 1–9. https://doi.org/10.1155/2011/619310.

Abdulrahman, S.A.M., Basavaiah, K., 2011b. Sensitive and selective spectrophotometric assay of gabapentin in capsules using sodium 1, 2-naphthoquinone-4-sulfonate. Drug Test. Anal. 3, 748–754. https://doi.org/10.1002/dta.242.

Abdulrahman, S.A.M., Basavaiah, K., 2012. Highly sensitive spectrophotometric method for the determination of gabapentin in capsules using sodium hypochloride. Turkish J. Pharm. Sci. 9, 113–126.

Adam, M.E., Shantier, S.W., Reem, S., Mohamed, M.A., Gadkariem, E.A., 2016. Development of Colorimetric Method for Determination of Gabapentin Using Ascorbic Acid as Chromogen. J. Chem. Pharm. Res. 8, 131–135.

Al-abadi, A.N., Rassol, A.A.A., 2011. Preparation and in-vitro evaluation of floating microspheres of gabapentin. Kufa J. Vet. Med. Sci. 2, 77–92.

Aleo, M., Ross, S., Becskei, C., Coscarelli, E., King, V., Darling, M., Lorenz, J., 2018. Palatability testing of oral Chewables in veterinary medicine for dogs. Open J. Vet. Med. 107–118. https://doi.org/10.4236/ojvm.2018.88011.

Almasri, I.M., Ramadan, M., Algharably, E., 2019. Development and validation of spectrophotometric method for determination of gabapentin in bulk and pharmaceutical dosage forms based on Schiff base formation with salicylaldehyde. J. Appl. Pharm. Sci. 9, 21–26. https://doi.org/10.7324/JAPS.2019.90304.

Andriotis, E.G., Eleftheriadis, G.K., Karavasili, C., Fatouros, D.G., 2020. Development of bio-active patches based on Pectin for the treatment of Ulcers and wounds using 3D-bioprinting technology. Pharmaceutics 12, 56. https://doi.org/10.3390/pharmaceutics12010056.

Anis, S.M., Hosny, M.M., Abdellatef, H.E., El-Balkiny, M.N., 2011. Spectrscopic and conductometric analysis of gabapentin. E-Journal Chem. 8, 1784–1796. https://doi.org/10.1155/2011/190517.

Arora, P., Sethi, V.Arora, TABLETS, ORODISPERSIBLE, 2013. A comprehensive review. Int. J. Res. Dev. Pharm. Life Sci. 2, 270–284.

Bali, A., Gaur, P., 2011. A novel method for spectrophotometric determination of pregabalin in pure form and in capsules. Chem. Cent. J. 5, 59. https://doi.org/10.1186/1752-153X-5-59.

Bhusnure, O.G., Yeote, N.S., Shete, R.S., Gholve, S.B., Giram, P.S., 2018. Formulation and evaluation of oral fast dissolving film of gabapentin by QBD approach. Int. J. Pharm. Biol. Sci. 8, 426–437. https://doi.org/10.20959/wjpr20177-8835.

Bittner, S.M., Smith, B.T., Diaz-Gomez, L., Hudgins, C.D., Melchiorri, A.J., Scott, D.W., Fisher, J.P., Mikos, A.G., 2019. Fabrication and mechanical characterization of 3D printed vertical uniform and gradient scaffolds for bone and osteochondral tissue engineering. Acta Biomater 90, 37–48. https://doi.org/10.1016/J.ACTBIO.2019.03.041.

Braga, D., Grepioni, F., Maini, L., Rubini, K., Polito, M., Brescello, R., Cotarca, L., Duarte, M.T., André, V., Piedade, M.F.M., 2008. Polymorphic gabapentin: thermal behaviour, reactivity and interconversion of forms in solution and solid-state. New J. Chem. 32, 1788–1795. https://doi.org/10.1039/b809662g.

Brannagan, T.H., 2009. Neuropathic pain. In: Rowland, L.P., Pedley, T. (Eds.), Merritt's Neurol. Wolters Kluwer, Philadelphia, pp. 838–843, 12th ed.

Chandra Dinda, S., Desireddy, R.B., Jitendrakumar, P., Narisireddy, P., Srimannarayana, K., Balaji, G.Jai, 2012. Development and validation of UV spectrophotometric method for estimation of agomelatine in bulk and pharmaceutical dosage form. Der Pharm. Lett. 3, 60–63.

Cheng, Y., Qin, H., Acevedo, N.C., Jiang, X., Shi, X., 2020. 3D printing of extended-release tablets of theophylline using hydroxypropyl methylcellulose (HPMC) hydrogels. Int. J. Pharm. 591, 119983 https://doi.org/10.1016/J.IJPHARM.2020.119983.

Ching, T., Li, Y., Karyappa, R., Ohno, A., Toh, Y.C., Hashimoto, M., 2019. Fabrication of integrated microfluidic devices by direct ink writing (DIW) 3D printing. Sensors Actuators B Chem 297, 126609. https://doi.org/10.1016/J.SNB.2019.05.086.

Conceição, J., Farto-Vaamonde, X., Goyanes, A., Adeoye, O., Concheiro, A., Cabral-Marques, H., Sousa Lobo, J.M., Alvarez-Lorenzo, C., 2019. Hydroxypropyl-β-cyclodextrin-based fast dissolving carbamazepine printlets prepared by semisolid

extrusion 3D printing. Carbohydr. Polym. 221, 55–62. https://doi.org/10.1016/j.carbpol.2019.05.084.
Croitoru-Sadger, T., Mizrahi, B., Yogev, S., Shabtay-Orbach, A., 2019. Two-component cross-linkable gels for fabrication of solid oral dosage forms. J. Control. Release. 303, 274–280. https://doi.org/10.1016/J.JCONREL.2019.04.021.
Cui, M., Yang, Y., Jia, D., Li, P., Li, Q., Chen, F., Wang, S., Pan, W., Ding, P., 2019. Effect of novel internal structures on printability and drug release behavior of 3D printed tablets. J. Drug Deliv. Sci. Technol. 49, 14–23. https://doi.org/10.1016/J.JDDST.2018.10.037.
Cui, M., Pan, H., Fang, D., Qiao, S., Wang, S., Pan, W., 2020. Fabrication of high drug loading levetiracetam tablets using semi-solid extrusion 3D printing. J. Drug Deliv. Sci. Technol. 57, 101683 https://doi.org/10.1016/J.JDDST.2020.101683.
Cutrignelli, A., Denora, N., Lopedota, A., Trapani, A., Laquintana, V., Latrofa, A., Trapani, G., Liso, G., 2007. Comparative effects of some hydrophilic excipients on the rate of gabapentin and baclofen lactamization in lyophilized formulations. Int. J. Pharm. 332, 98–106. https://doi.org/10.1016/j.ijpharm.2006.09.053.
Dahiya, J., Jalwal, P., Singh, B., 2015. Chewable Tablets: a Comprehensive Review. Pharma Innov. J 4 (5), 100–105. www.thepharmajournal.com.
Davidson, G., 2017. Veterinary compounding: regulation, challenges, and resources. Pharmaceutics 9, 5. https://doi.org/10.3390/pharmaceutics9010005.
Dores, F., Kuźmińska, M., Soares, C., Bohus, M., Shervington, L.A., Habashy, R., Pereira, B.C., Peak, M., Isreb, A., Alhnan, M.A., 2020. Temperature and solvent facilitated extrusion based 3D printing for pharmaceuticals. Eur. J. Pharm. Sci. 152, 105430 https://doi.org/10.1016/J.EJPS.2020.105430.
Eduardo, D.T., Ana, S.E., José B, F., 2021. A micro-extrusion 3D printing platform for fabrication of orodispersible printlets for pediatric use. Int. J. Pharm 605, 120854. https://doi.org/10.1016/J.IJPHARM.2021.120854.
Eisenstein, M., 2015. First 3D-printed pill. Nat. Biotechnol 22, 1014. https://doi.org/10.1038/nbt1015-1014a.
El Aita, I., Breitkreutz, J., Quodbach, J., 2019. On-demand manufacturing of immediate release levetiracetam tablets using pressure-assisted microsyringe printing. Eur. J. Pharm. Biopharm. 134, 29–36. https://doi.org/10.1016/J.EJPB.2018.11.008.
El Aita, I., Breitkreutz, J., Quodbach, J., 2020. Investigation of semi-solid formulations for 3D printing of drugs after prolonged storage to mimic real-life applications. Eur. J. Pharm. Sci. 146, 105266 https://doi.org/10.1016/J.EJPS.2020.105266.
Elbl, J., Gajdziok, J., Kolarczyk, J., 2020. 3D printing of multilayered orodispersible films with in-process drying. Int. J. Pharm. 575, 118883 https://doi.org/10.1016/j.ijpharm.2019.118883.
European Pharmacopoeia Commission, 2020a. 2.9.1. Disintegration of Tablets and capsules, in: Eur. Pharmacopoeia, 10.0, European Directorate For the Quality of Medicines (EDQM), Strasbourg, France, pp. 323–325.
European Pharmacopoeia Commission, 2020b. 2.9.3. Dissolution Test For Solid Dosage forms, in: Eur. Pharmacopoeia, 10.0, European Directorate For the Quality of Medicines (EDQM), Strasbourg, France, pp. 326–333.
Everett, H., 2021. 3D Print. Ind.
FDA, C.D.E.R., 2018. Quality attribute considerations for chewable tablets guidance for industry. Silver Spring, MD.
Fonseca, F., Brito de Barros, R., Ilharco, L.M., Garcia, A.R., 2017. Spectroscopic methods for quantifying gabapentin: framing the methods without derivatization and application to different pharmaceutical formulations. Appl. Spectrosc 71, 2519–2531. https://doi.org/10.1177/0003702817716181.
Galande, V.R., Baheti, K.G., Dehghan, M.H., 2010. UV-Vis spectrophotometric method for estimation of Gabapentin and Methylcobalamin in bulk and tablet. Int. J. ChemTech Res. 2, 695–699.
Golden Gate Veterinary Compounding Pharmacy, (n.d.). https://ggvcp.pharmacy/(accessed February 11, 2022).
Goswami, A., Jiang, J.-.Q., 2018. Simultaneous quantification of Gabapentin, Sulfamethoxazole, Terbutryn, Terbuthylazine and Diuron by UV-Vis spectrophotometer. Biointerface Res. Appl. Chem. 8, 3111–3117.
Gouda, A.A., Al Malah, Z., 2013. Development and validation of sensitive spectrophotometric method for determination of two antiepileptics in pharmaceutical formulations. Spectrochim. Acta - Part A Mol. Biomol. Spectrosc. 105, 488–496. https://doi.org/10.1016/j.saa.2012.12.053.
Goyanes, A., Madla, C.M., Umerji, A., Duran Piñeiro, G., Giraldez Montero, J.M., Lamas Diaz, M.J., Gonzalez Barcia, M., Taherali, F., Sánchez-Pintos, P., Couce, M.L., Gaisford, S., Basit, A.W., 2019. Automated therapy preparation of isoleucine formulations using 3D printing for the treatment of MSUD: first single-centre, prospective, crossover study in patients. Int. J. Pharm. 567, 118497 https://doi.org/10.1016/J.IJPHARM.2019.118497.
Gujral, R.S., Haque, S.M., Shanker, P., 2009. A sensitive UV spectrophotometric method for the determination of gabapentin. E-Journal Chem 6, 163–171. https://doi.org/10.1155/2009/451967.
Haring, A.P., Tong, Y., Halper, J., Johnson, B.N., 2018. Programming of multicomponent temporal release profiles in 3D printed Polypills via Core–Shell, multilayer, and gradient concentration profiles. Adv. Healthc. Mater. 7, 1–10. https://doi.org/10.1002/adhm.201800213.
Herrada-Manchón, H., Rodríguez-González, D., Alejandro Fernández, M., Suñé-Pou, M., Pérez-Lozano, P., García-Montoya, E., Aguilar, E., 2020. 3D printed gummies: personalized drug dosage in a safe and appealing way. Int. J. Pharm. 587, 119687 https://doi.org/10.1016/J.IJPHARM.2020.119687.
Jaipal, A., Pandey, M.M., Charde, S.Y., Raut, P.P., Prasanth, K.V., Prasad, R.G., 2015. Effect of HPMC and mannitol on drug release and bioadhesion behavior of buccal discs of buspirone hydrochloride: in-vitro and in-vivo pharmacokinetic studies. Saudi Pharm. J. 315–326. https://doi.org/10.1016/j.jsps.2014.11.012.
Karavasili, C., Gkaragkounis, A., Moschakis, T., Ritzoulis, C., Fatouros, D.G., 2020. Pediatric-friendly chocolate-based dosage forms for the oral administration of both hydrophilic and lipophilic drugs fabricated with extrusion-based 3D printing. Eur. J. Pharm. Sci. 147, 105291 https://doi.org/10.1016/J.EJPS.2020.105291.
Kazemipour, M., Fakhari, I., Ansari, M., 2013. Gabapentin determination in human plasma and capsule by coupling of solid phase extraction, derivatization reaction, and UV-vis spectrophotometry. Iran. J. Pharm. Res. 12, 247–253. https://doi.org/10.22037/ijpr.2013.1347.
Kostić, N., Dotsikas, Y., Malenović, A., 2014. Critical review on the analytical methods for the determination of zwitterionic antiepileptic drugs-Vigabatrin, Pregabalin, and Gabapentin - In bulk and formulations. Instrum. Sci. Technol. 42, 486–512. https://doi.org/10.1080/10739149.2013.876545.
Lamichhane, S., Park, J.-.B., Sohn, D.H., Lee, S., 2019. Customized novel design of 3D printed pregabalin tablets for intra-gastric floating and controlled release using fused deposition modeling. Pharmaceutics 11, 564.
Lin, S.Y., Hsu, C.H., Ke, W.T., 2010. Solid-state transformation of different gabapentin polymorphs upon milling and co-milling. Int. J. Pharm. 396, 83–90. https://doi.org/10.1016/j.ijpharm.2010.06.014.
Liu, J., Tagami, T., Ozeki, T., 2020a. Fabrication of 3D-printed fish-gelatin-based polymer hydrogel patches for local delivery of pegylated liposomal doxorubicin. Mar. Drugs. 18 https://doi.org/10.3390/md18060325.
Liu, K., Zhu, L., Tang, S., Wen, W., Lu, L., Liu, M., Zhou, C., Luo, B., 2020b. Fabrication and evaluation of a chitin whisker/poly (L-lactide) composite scaffold by the direct trisolvent-ink writing method for bone tissue engineering. Nanoscale 12, 18225. https://doi.org/10.1039/d0nr04204h.
Mathews, K., Kronen, P.W., Lascelles, D., Nolan, A., Robertson, S., Steagall, P.V.M., Wright, B., Yamashita, K., 2014. Guidelines for recognition, assessment and treatment of pain. J. Small Anim. Pract. 55, 10–68.
McDevitt, J.T., Gurst, A.H., Chen, Y., 1998. Accuracy of Tablet Splitting. Pharmacotherapy. 18, 193–197. https://doi.org/10.1002/j.1875-9114.1998.tb03838.x.
Mohammed, T.A., Mohamed, M.A., 2015. Spectrophotometric determination of certain antiepileptic's in tablets using vanillin reagent. J. Adv. Chem. 11, 3540–3551.
Moosavi, S.M., Ghassabian, S. Linearity of calibration curves for analytical methods: a review of criteria for assessment of method reliability, in: M. Stauffer (Ed.), Calibration Valid. Anal. Methods - A Sampl. Curr. Approaches, IntechOpen, 2018: pp. 109–127. doi:10.5772/intechopen.72932.
Nair, A.B., Kumria, R., Harsha, S., Attimarad, M., Al-Dhubiab, B.E., Alhaider, I.A., 2013. In vitro techniques to evaluate buccal films. J. Control. Release. 166, 10–21. https://doi.org/10.1016/j.jconrel.2012.11.019.
Noor, N., Shapira, A., Edri, R., Gal, I., Wertheim, L., Dvir, T., 2019. 3D printing of personalized thick and Perfusable cardiac patches and hearts. Adv. Sci. 6, 1900344 https://doi.org/10.1002/advs.201900344.
Norman, J., Madurawe, R.D., Moore, C.M.V., Khan, M.A., Khairuzzaman, A., 2017. A new chapter in pharmaceutical manufacturing: 3D-printed drug products. Adv. Drug Deliv. Rev. 108, 39–50. https://doi.org/10.1016/j.addr.2016.03.001.
Nyamweya, N.N., Kimani, S.N., 2020. Chewable tablets: a review of formulation considerations. Pharm. Technol. 44, 38–44.
Ranjous, Y., Hsian, J., 2013. Improvement in the physical and chemical stability of gabapentin by using different excipients. Int. J. Pharm. Sci. Rev. Res. 23, 81–86.
Rasoulianboroujeni, M., Fahimipour, F., Shah, P., Khoshroo, K., Tahriri, M., Eslami, H., Yadegari, A., Dashtimoghadam, E., Tayebi, L., 2019. Development of 3D-printed PLGA/TiO2 nanocomposite scaffolds for bone tissue engineering applications. Mater. Sci. Eng. C 96, 105–113. https://doi.org/10.1016/J.MSEC.2018.10.077.
Rycerz, K., Stepien, K.A., Czapiewska, M., Arafat, B.T., Habashy, R., Isreb, A., Peak, M., Alhnan, M.A., 2019. Embedded 3D printing of novel bespoke soft dosage form concept for pediatrics. Pharmaceutics 11, 630. https://doi.org/10.3390/pharmaceutics11120630.
Salem, H., 2008. Analytical study for the charge-transfer complexes of gabapentin. African J. Pharm. Pharmacol. 2, 136–144.
Sayare, A.S., Pithe, A.R., Ghode, P.D., Khandelwal, K.R., 2019. Formulation and evaluation of gabapentin loaded chitosan transdermal films. J. Pharm. Sci. Res. 11, 2872–2877. https://doi.org/10.22159/ijap.2019v11i3.31932.
Siddiqui, F.A., Arayne, M.S., Sultana, N., Qureshi, F., Mirza, A.Z., Zuberi, M.H., Bahadur, S.S., Afridi, N.S., Shamshad, H., Rehman, N., 2010. Spectrophotometric determination of gabapentin in pharmaceutical formulations using ninhydrin and π-acceptors. Eur. J. Med. Chem. 45, 2761–2767. https://doi.org/10.1016/j.ejmech.2010.02.058.
Siddiqui, F.A., Sher, N., Shafi, N., Shamshad, H., Zubair, A., 2013. Kinetic and thermodynamic spectrophotometric technique to estimate gabapentin in pharmaceutical formulations using ninhydrin. J. Anal. Sci. Technol. 4, 1–8. https://doi.org/10.1186/2093-3371-4-17.
Siyawamwaya, M., du Toit, L.C., Kumar, P., Choonara, Y.E., Kondiah, P.P.P.D., Pillay, V., 2019. 3D printed, controlled release, tritherapeutic tablet matrix for advanced anti-HIV-1 drug delivery. Eur. J. Pharm. Biopharm. 138, 99–110. https://doi.org/10.1016/J.EJPB.2018.04.007.
Sjöholm, E., Sandler, N., 2019. Additive manufacturing of personalized orodispersible warfarin films. Int. J. Pharm. 564, 117–123. https://doi.org/10.1016/j.ijpharm.2019.04.018.
Sjöholm, E., Mathiyalagan, R., Prakash, D.R., Lindfors, L., Wang, Q., Wang, X., Ojala, S., Sandler, N., 2020. 3D-Printed veterinary dosage forms—a comparative study of three semi-solid extrusion 3D printers. Pharmaceutics 12, 1239. https://doi.org/10.3390/pharmaceutics12121239.
Tagami, T., Ando, M., Nagata, N., Goto, E., Yoshimura, N., Takeuchi, T., Noda, T., Ozeki, T., 2019. Fabrication of Naftodipid-Loaded Tablets Using a Semisolid Extrusion-Type 3D printer and the Characteristics of the Printed Hydrogel and Resulting Tablets. J. Pharm. Sci. 108, 907–913. https://doi.org/10.1016/j.xphs.2018.08.026.

Tagami, T., Ito, E., Kida, R., Hirose, K., Noda, T., Ozeki, T., 2021. 3D printing of gummy drug formulations composed of gelatin and an HPMC-based hydrogel for pediatric use. Int. J. Pharm. 594, 120118 https://doi.org/10.1016/J.IJPHARM.2020.120118.

Taylor, C.P., 2002. Gabapentin mechanisms of action. In: Levy, R., M., R., Meldrum, B., Perucca, E. (Eds.), Antiepileptic Drugs, 5th Ed. Wolters Kluwer Health, Philadelphia, pp. 319–360.

U.S. Department of Health and Human Services Food and Drug Administration Center for Drug Evaluation and Reseach, 2018. Dissolution testing and acceptance criteria for immediate-release solid oral dosage form drug products containing high solubility drug substances - guidance for industry. FDA Biopharm. http://www.fda.gov/Drugs/GuidanceComplianceRegulatoryInformation/Guidances/default.htm%0Afile:///C:/Users/ASUS/Desktop/RujukanPhD/DrugRelease/1074043FNL_clean.pdf.

U.S. Food and Drug Administration, Statement by FDA Commissioner Scott Gottlieb, M. D., on FDA ushering in new era of 3D printing of medical products; provides guidance to manufacturers of medical devices, FDA. (2017). https://www.fda.gov/news-events/press-announcements/statement-fda-commissioner-scott-gottlieb-md-fda-ushering-new-era-3d-printing-medical-products (accessed February 28, 2022).

Wedgewood Pharmacy, (n.d.). https://www.wedgewoodpharmacy.com/(accessed February 11, 2022).

Williams, M. The Merck Index: an Encyclopedia of Chemicals, Drugs, and Biologicals, 15th Edition-Edited by M.J. O'Neil, Drug Dev. Res. 74 (2013) 339. doi:10.1002/ddr.21085.

Wu, M., Zhang, Y., Huang, H., Li, J., Liu, H., Guo, Z., Xue, L., Liu, S., Lei, Y., 2020. Assisted 3D printing of microneedle patches for minimally invasive glucose control in diabetes. Mater. Sci. Eng. C. 117, 111299 https://doi.org/10.1016/J.MSEC.2020.111299.

Yan, T.T., Lv, Z.F., Tian, P., Lin, M.M., Lin, W., Huang, S.Y., Chen, Y.Z., 2020. Semi-solid extrusion 3D printing ODFs: an individual drug delivery system for small scale pharmacy. Drug Dev. Ind. Pharm. 46, 531–538. https://doi.org/10.1080/03639045.2020.1734018.

Yang, Y., Wang, X., Lin, X., Xie, L., Ivone, R., Shen, J., Yang, G., 2020a. A tunable extruded 3D printing platform using thermo-sensitive pastes. Int. J. Pharm. 583, 119360 https://doi.org/10.1016/J.IJPHARM.2020.119360.

Yang, Y., Wang, K., Liu, D., Zhao, X., Fan, J., 2020b. Effects of land-use conversions on the ecosystem services in the agro-pastoral ecotone of northern China. J. Clean. Prod. 249, 119360 https://doi.org/10.1016/J.JCLEPRO.2019.119360.

Zheng, Z., Lv, J., Yang, W., Pi, X., Lin, W., Lin, Z., Zhang, W., Pang, J., Zeng, Y., Lv, Z., Lao, H., Chen, Y., Yang, F., 2020. Preparation and application of subdivided tablets using 3D printing for precise hospital dispensing. Eur. J. Pharm. Sci. 149, 105293 https://doi.org/10.1016/J.EJPS.2020.105293.

Zhou, L., Ramezani, H., Sun, M., Xie, M., Nie, J., Lv, S., Cai, J., Fu, J., He, Y., 2020. 3D printing of high-strength chitosan hydrogel scaffolds without any organic solvents †. Biomater. Sci 8, 5020. https://doi.org/10.1039/d0bm00896f.

Zong, Z., Desai, S.D., Kaushal, A.M., Barich, D.H., Huang, H.S., Munson, E.J., Suryanarayanan, R., Kirsch, L.E., 2011. The stabilizing effect of moisture on the solid-state degradation of gabapentin. AAPS PharmSciTech 12, 924–931. https://doi.org/10.1208/s12249-011-9652-8.